Single-molecule DNA unzipping reveals asymmetric modulation of the transcription factor Egr-1 by its binding site sequence and context

Sergei Rudnizky[1,2,*], Hadeel Khamis[1,3,*], Omri Malik[1,2], Allison Squires[4,6], Amit Meller[2,4,5], Philippa Melamed[1,2] and Ariel Kaplan[1,2,#]

[1]Faculty of Biology, Technion – Israel Institute of Technology, Haifa (32000), Israel

[2]Russell Berrie Nanotechnology Institute, Technion – Israel Institute of Technology, Haifa (32000), Israel

[3]Faculty of Physics, Technion – Israel Institute of Technology, Haifa (32000), Israel

[4]Department of Biomedical Engineering, Boston University, Boston, MA 02215, USA

[5]Faculty of Biomedical Engineering, Technion – Israel Institute of Technology, Haifa (32000), Israel

[6]Present address: Department of Chemistry, Stanford University, Stanford, CA 94305

* These authors contributed equally to this work

#To whom correspondence should be addressed;

email: akaplanz@technion.ac.il

Abstract

Binding of transcription factors to regulatory elements is a central step in the complex regulation of gene expression, and its perturbation is linked to numerous disease states. Egr-1 is an inducible transcription factor that binds to 9-bp response elements via three zinc finger domains in response to a variety of stimuli, such as hormonal signals and stress. In our work, we use single-molecule DNA unzipping with optical tweezers to study the binding properties of Egr-1 to its binding sites, using as a model the promoter of the *Lhb* gene. We find that both the core 9 base pairs bound to Egr-1 in each of the binding sites on *Lhb*, and the base pairs flanking these sites, modulate the affinity and structure of the protein-DNA complex. The effect of the flanking sequences is asymmetric, with a stronger effect for the sequence flanking the triplet in contact with zinc finger 3. Next, using a novel method to characterize the dissociation time of Egr-1 at the single molecule level, we show that a local, mechanical perturbation of the interactions of zinc finger 3 is able to destabilize the complex more effectively than a similar perturbation acting on the interactions of ZF1. Taken together, our findings suggest a novel functional role for ZF3 in the interaction of Egr-1 with other proteins.

Introduction

Binding of Transcription Factors (TFs) to regulatory elements at the promoters and enhancers of genes is a central event in the regulation of transcription, and lies at the core of the cell's response to environmental stimuli. As such, a detailed understanding of the interactions of TFs with DNA is crucial, not only at "large" scales, e.g. identifying TF binding sites throughout genomes(1–3), but also at the "small" scale, by developing a molecular understanding of the different factors affecting the structure and dynamics of the TF-DNA complex, and how it affects transcriptional regulation. Recent studies have highlighted the existence of multiple layers of complexity in the modulation of a TF binding to DNA, revealing the effects of the structure and flexibility of the binding site(4, 5), the kinetic competition of TFs with nucleosomes(6–8), cooperativity between TFs(9–13), the presence of neighboring TF sites(14, 15), and DNA methylation(16). However, the diversity of mechanisms by which TFs select *in vivo* binding sites and alter gene expression remain unclear, calling for a mechanistic understanding of all these factors to understand TF function.

Egr-1 (also known as zif268) is a TF responsible for the regulation of a variety of genes, and is induced by various stimulants, such as growth factors(17), neurotransmitters(18), hormones(19, 20), and stress(21). Previous studies have established a 9 bp 'GCGTGGGCG' consensus binding motif for Egr-1(22). A crystal structure of the protein bound to this motif shows that Egr-1 binds this recognition sequence as a monomer via interactions of its three zinc fingers (ZF1, ZF2 and ZF3), which contact 3 bp of DNA each(23). The wide interface created by the ZFs when bound to DNA, provide a strong, stable and specific binding. Upon stimulation, the levels of Egr-1 are estimated to rise up to $\sim 10^4$ copies per nucleus(24, 25), but its lifetime is limited to ~1 h(25) . Hence, in order to activate gene expression and respond to its stimulus, Egr-1 needs to rapidly scan the DNA in search for its response elements. During this search process, Egr-1 is required to discriminate its target site from among billions of bases, within a time frame of minutes. As a result, a tight binding conformation, like the one described above, can prevent the protein from efficiently scanning the genome, since many molecular bonds would need to be constantly created and disrupted. These seemingly contradictory requirements, of a stable configuration at the recognition element but a loosely bound one at non-specific DNA, has been named the 'speed-stability' paradox(26). Recent studies using NMR spectroscopy helped to resolve it, revealing a surprisingly different protein structure of Egr-1 while bound to non-specific DNA(27). In this conformation, ZF3 and ZF2 are bound to DNA, but ZF1 undergoes rapid dissociations. It was proposed that Egr-1 exploits this lower-affinity 'scanning' conformation in order to rapidly diffuse on the DNA, until it encounters its recognition sequence, binding to which traps the protein in the 'recognition mode' observed in the crystal structure. However, binding sites in real, transcribed genes do not exhibit in general the consensus sequence. In fact, many of these sites show gene-specific and evolutionary-conserved deviations from the consensus[REF], indicating that the specific type of interactions Egr-1 makes with its binding

elements have a functional importance. Hence, elucidating how the structure and dynamics of the Egr-1 complex is modulated by the binding site sequence and its genomic context is of great interest. Moreover, it is predicted that the mammalian genome harbors ~10^6 sites that are highly similar, but not identical, to the classical recognition sequence of Egr-1(28, 29). Most of these sites, without a regulatory role, are expected to affect the search process, as they can momentarily trap Egr-1(30). The role of such sites is thought to be negative when these sequences are located relatively far from the target sequence, or positive if they are located in the vicinity of the response element where they help increase the protein's local concentration(14, 15). Unfortunately, since most of the experiments have concentrated on the consensus sequence, it is not clear how Egr-1 binds to the variable ones. Interestingly, a thermodynamic additivity model was proposed to predict the affinity of near-consensus sites, but it was found to fail for sequences with four or more substitutions(31).

Two Egr-1 response elements reside ~60 bp apart within the evolutionary conserved proximal segment of the Luteinizing Hormone beta subunit (*Lhb*) gene promoter. In gonadotrope cells, Egr-1 is induced by the Gonadotropin Releasing Hormone (GnRH) to regulate the expression of the *Lhb* gene, and is essential for GnRH-induced gene activation and fertility in mice(32). Interestingly, both Egr-1 binding elements are different from the consensus motif, and they also differ by 4 bp from each other. These variations are conserved among the species (Supplementary Fig. 1), suggesting a functional role. Moreover, sequences flanking these sites are evolutionary conserved too, suggesting also that the DNA content surrounding these sites is important.

It has been shown that DNA unzipping using single-molecule optical tweezers can provide a direct measurement of the position and forces associated with proteins bound to DNA(33–35), thus overcoming the limitations of traditional ensemble methods with their inherent averaging. In our work, we used this methodology to unzip the *Lhb* promoter in the presence of the DNA binding domain of Egr-1, thus measuring the occupancy and forces associated with Egr-1 binding to its response elements in their native context. We then compared these results with those obtained when the individual binding sites were located in other DNA contexts. Finally, we used a novel method to characterize the dissociation time of Egr-1 from its binding site, under asymmetric perturbations of the underlying DNA. Our results indicate that each of the functional binding sites, and their native flanking sequences, modulate the structure and affinity of the Egr-1-DNA complex in a different way, and suggest a unique functional role for ZF3 contacts with DNA.

Results

Single-molecule probing of Egr-1 binding reveals distinct structural conformations

Two putative binding sites for Egr-1, with sequence CACCCCCAC and CGCCCCCAA, are located, respectively, at positions -41/-49 and -104/-112 on the mouse *Lhb* gene, and are both important for its induction in gonadotrope cells. These sites are

remarkably conserved among the species despite a number of introduced substitutions which diverge from the consensus motif (Supplementary Fig. 1). To characterize the binding of Egr-1 to each of these sites in its native DNA context, we subjected the -517/+247 bp region of *Lhb* to single-molecule analysis by DNA unzipping. We attached each of the two DNA strands at the -517 end of the *Lhb* DNA to a ~ 2000-bp DNA 'handle' harboring a tag (Biotin and Digoxygenin, respectively), thus allowing to tether the DNA construct between two ~1 micro-meter microspheres (covered with streptavidin and anti-digoxygenin, respectively), trapped in a high-resolution, dual trap optical tweezers setup (Figs. 1a,b). Then, we subjected the construct to mechanical force by moving one of the traps away from the other. When the applied forces reached ~16-17 pN, the sample DNA unzipped, as evidenced by a reproducible pattern of events that include a sudden decrease in force together with an increase in extension. It has been previously shown(33–35) that following the propagation of the unzipping fork allows to measure the position and strength of protein-DNA interactions, as the force required to disrupt these interactions is significantly higher than those needed to disrupt DNA alone. Hence, using a laminar flow system, we exposed our construct to a solution containing the DNA binding domain of Egr-1 (referred to as Egr-1 for simplicity), and unzipped the DNA in its presence. As expected, a clear force elevation was observed in the positions proximal to ~-41/-49 (site -1) and -104/-112 (site -2), indicating binding of Egr-1 to these sites (Fig. 1c, Supplementary Fig. 2a). Surprisingly, an additional force peak was detected in the position surrounding ~-360 (site -3). When we analyzed the sequence of the DNA at this position, it was clear that it corresponds to an additional putative binding site located between -349/-358, which corresponds to GGCCCACTC, a motif with two base substitutions as compared to the 9 bp consensus, and different by 3-4 bp from the other Egr-1 binding sequences located on the *Lhb* promoter. The force peaks detected for the three sites were not observed in the absence of Egr-1 (Fig. 1d, Supplementary Fig. 2b), nor for a control DNA sequence that does not harbor any known Egr-1 binding sites. Moreover, although the experiment was performed at a high concentration of protein (500 nM), at which a significant amount of it will be bound to DNA non-specifically, the measured forces in non-specific regions were identical in the presence or absence of the TF, suggesting that the forces required to disrupt the non-specific complexes are significantly lower than those required to disrupt Egr-1 from specific sites. In addition, to evaluate whether peaks detected in successive unzipping cycle for a single molecule correspond to new binding events following each unzipping cycle, we performed the following control experiment: We first unzipped the DNA, thus disrupting Egr-1 binding, and then moved into a flow channel that does not contain Egr-1, relaxed the tension to allow reannealing of double stranded DNA (dsDNA), and immediately unzipped the DNA again. No proteins were found bound to DNA, in any of the binding sites, in the second unzipping cycle of these experiments (n=10).

Accordingly, unzipping DNA multiple times in the presence of Egr-1, allowed us to calculate the mean breaking force (Fig. 1e) as well as the fraction of successive Egr-1 binding events, out of the total number of unzipping cycles (i.e. the binding probability; Fig. 1f), for each DNA molecule for each of the three sites. Remarkably,

these experiments revealed significant differences in the binding probability, between each of the three sites: Egr-1 was found bound to site-1 with the highest probability, as compared to both -2 ($p<0.001$) and -3 ($p<2x10-8$) sites. Assuming that the binding reaction reaches equilibrium, the binding frequency measured in these experiments should reflect the affinity of Egr-1 for a particular DNA sequence(36). It was previously shown that the affinity of Egr-1 to site -1 is higher than that to site -2 and lower than the affinity of the Egr-1 consensus sequence(37), which is consistent with our results. Next, to further clarify the differences in affinity between the different sites, we repeated these experiments in the presence of various concentrations of Egr-1. It has been shown that the consensus sequence exhibits the highest affinity of Egr-1 to DNA(29). Therefore, in addition to *Lhb* DNA, we performed the same experiment with the consensus sequence, introduced into a DNA segment derived from the 601 nucleosome positioning (context C1, Supplementary Fig. 3). For all the four sites probed, the binding probability is consistent with a hyperbolic saturation curve, as function of protein concentration (Supplementary Fig. 4a), from which the affinity of Egr-1 for a specific site can be estimated (Supplementary Table 8). As expected, the affinity for the consensus sequence was the highest, as compared with the sites located on *Lhb*, with similar affinities for sites -1 and -3, and lowest for site -2.

Interestingly, we found that the mean breaking forces (Fig. 1e, Supplementary Fig. 2c-e) are not correlated with the binding probabilities: For example, although the binding probability for site -3 was significantly lower than that of site -1, the mean breaking force for site -3 was significantly higher ($p<10^{-28}$). In addition, the mean breaking force did not show a concentration dependence (Supplementary Fig. 4b), suggesting that it is an intrinsic property of each site. Importantly, while the binding probability at equilibrium is expected to depend only on the protein's binding energy, the magnitude of the breaking force measured in these unzipping experiments depends on the *shape* of the energy landscape for the mechanical disruption reaction, which depends on the structure of the protein-DNA complex. As a result, differences in breaking force can reflect differences in structure, even if the different structures have similar affinities. Hence, the breaking forces we observed for the three binding sites on *Lhb*, which are uncorrelated with their binding probability, suggest that Egr-1 binds each of these sequence motifs in a significantly different structural conformation.

Previous studies suggested that the presence of an additional binding site proximal to a given site, can reduce its binding probability, as each site will compete with the other for protein binding. Since site -1 and site -2 are positioned only ~60 bp away from each other, we checked whether binding to each of these sites affects binding to the other. To that end we calculated the conditional probability of detecting a protein at a given site, given that there is a protein at the second. When we compared unconditional with conditional binding probability of both sites, we did not observe any significant difference between them (Supplementary Fig. 5).

Flanking sequences proximal to zinc finger 3 modulate Egr-1 binding

The observed breaking force and binding probability of each single site was

measured in the context of others sites *in cis*. This made us wonder whether the observed differences are solely due to the identity (i.e. the sequence) of the core 9 bp sequence of each site, or also affected by the sequence context. To that end, we introduced the 9 bp motif corresponding to each of the three sites, separately, into the same flanking context of C1 (Supplementary Fig. 3), and subjected them to multiple rounds of unzipping in presence of Egr-1 (Fig. 2). These experiments revealed that, although the binding probability of site -1 was unchanged as compared to the one measured on *Lhb* (Fig. 2b), for site -2 it was significantly increased ($p=4x10^{-4}$) and for site -3 significantly reduced ($p=2x10^{-3}$). The breaking forces for site -1 and site -2 were significantly elevated, while for site -3 it was significantly reduced (Fig. 2a). Introducing the sites into a different flanking context (C2, Supplementary Fig. 3), showed a significantly different set of forces and binding probabilities (Fig. 2a,b). For example, the binding probability for site -3 in the C2 context is nearly equal to the one in the native *Lhb* context.

In order to understand the effect of the flanking sequences on Egr-1 binding, we used site -1 in the C1 context and mutated the first base proximal to the nucleotide triplet bound by ZF1 (base number -1). The crystal structure of Egr-1 shows that ZF1 can make hydrogen bonds with this base(38), thus it is possible that the observed changes in binding probability and breaking force upon change of DNA context, are due to the substitution of this specific nucleotide. Remarkably, unzipping experiments using the mutated flanking base at this position led to a mild decrease in breaking force, but showed no significant change in binding probability (Figs. 3a,b). In contrast, when we mutated the first nucleotide proximal to ZF3 (base number 10), a significant reduction in both breaking force and binding probability was observed (Fig. 3a,b). Interestingly, when we performed the same experiments with the consensus sequence, we did not observe significant changes in binding frequency or breaking force upon mutagenesis of base number 10, and a reduction in force but no change in binding probability for mutagenesis of base number -1 (Figs. 3c,d).

Previous studies have shown that 3-5 nucleotides surrounding to core binding site have a major effect on binding for some of TFs(39, 40). In addition, genome wide data suggests that Zinc-finger TFs of the C_2H_2 type prefer GC rich over the AT rich flanking sequences(41). Hence, to check whether the effect of flanking sequences can extend beyond the first nucleotide flanking the binding motif, we gradually mutated 8-11 nucleotides proximal to ZF1 or ZF3 of site -1, by replacing them with repeats of the AT di-nucleotides (Supplementary Fig. ???). The effect of replacement on breaking force was evident for some of the nucleotide substitutions flanking both ZF1 and ZF3 (Fig 4). However, only the change of base number 10, proximal to ZF3, significantly reduced both breaking force and binding probability. Collectively, these results suggest that, at least for naturally occurring Egr-1 binding sites, the flanking sequences proximal to ZF1 affect the structure of the protein-DNA complex, without a strong effect on its affinity, whilst the first nucleotide proximal to ZF3 controls both structure and affinity of Egr-1-DNA complex.

Local disruption of ZF3 reduces Egr-1 binding

The observed asymmetric effect of flanking nucleotides suggested that the region proximal to ZF3 plays an important role in Egr-1 binding. Previous studies proposed that Egr-1 can bind to DNA via two distinct conformations, the recognition mode where all its ZFs are bound to DNA, and a scanning mode in which only two ZFs are bound (27, 42). Thus, we hypothesized that the dramatic effect observed as a result of the substitution of the nucleotide proximal to the triplet bound by ZF3, may reflect a particular sensitivity of the Egr-1-DNA complex for the local perturbation of ZF3, modulating Egr-1 binding as a whole. If this is the case, we would expect that dissociation of Egr-1 from the DNA will require less force if the perturbation is from the ZF3 direction.

To test this hypothesis, we compared the previous experiments unzipping *Lhb* from the -517 end ("forward unzipping"), where the unzipping fork encounters ZF1 first on sites -1, -2 and -3, with experiments where we unzipped *Lhb* DNA from the +246 end ("reverse unzipping"), approaching Egr-1 from the direction of ZF3 (Fig 5a). Notably, the mean breaking force required to disrupt the protein from sites -1 and -2 was significantly reduced ($p<5X10^{-11}$ and $p<0.02$), as compared to the force required to disrupt it from the ZF1 orientation. Moreover, the force required for disruption of Egr-1 from site-3, that was the highest among the three sites in the forward unzipping, was so dramatically reduced, that we could not detect any force peak in the location near this site (Fig 5). This suggest that the sequence of the binding motif can modulate the specific interactions of the ZFs, creating different degrees of an asymmetric structure for sites -2 and -3, where ZF1 is more tightly associated with DNA than ZF3, as compared to the complex formed on site -1 where the interactions are nearly symmetric. (Of note, the significant reductions we observe for the binding probability are likely the result of more binding events that whose breaking force is close to the force sensitivity threshold set by the unzipping force of naked DNA, and are therefore missed). Surprisingly, two additional force peaks were detected in the positions previously unidentified inside the *Lhb* gene body (Supplementary Fig. 7). When we checked the identity of DNA sequence at the detected peaks, it was clear that they corresponded to the additional putative binding sites GAGTGGGTG and GAGGGGGTC at +113/+121 and +205/+213, respectively, downstream the TSS. Importantly, they are positioned in the opposite orientation as compared with sites -1,-2 and -3, so the unzipping fork first encounters ZF3 in these sites during "forward" unzipping.

Next, to further check whether perturbation of Egr-1 from the ZF3 direction is a site-specific property, or a more general property of the structure of the Egr-1-DNA complex, we reverse-unzipped the Egr-1-consensus complex. Consistent with the results for the naturally occurring sites, we observed a significant reduction in breaking force ($P<5x10^{-22}$) as compared to disruption from the ZF1 direction. These results suggest that the reduction in forces required for disruption of the protein through ZF3 is a general property that reflects Egr-1 binding to DNA.

Finally, we wanted to understand whether Egr-1 dissociation is faster upon local disruption of ZF3 compared ZF1. Accordingly, we mimicked a local disruption of each ZF by partially unzipping DNA from the forward direction (for disruption of

ZF1) or reverse direction (for disruption of ZF3). We unzipped the DNA until the fork reached the position of the consensus binding site, leaving it to rapidly fluctuate between a locally open (ssDNA) and locally closed (dsDNA) state (Fig. 6a,b). Next, we exploited our laminar flow cell to move the fluctuating DNA to the channel in which Egr-1 was present. Exposure of the DNA to the Egr-1 channel led to a quick transition of the DNA into a closed form, and a complete repression of the fluctuations, indicating Egr-1 binding. Reappearance of the fast fluctuations indicated dissociation of the protein. Multiple events of binding and dissociation could be observed for a single molecule with continuous exposure to Egr-1 (Supplementary Fig. 8c). To observe a single event of dissociation we moved the construct back to the channel in which Egr-1 was absent, to prevent re-binding. The time lapsed until the reappearance of fluctuations (Fig. 6b) allowed us to measure the characteristic dissociation time of single Egr-1 molecule under a tension applied on the ZF1 or ZF3 side. Remarkably, when we approached the consensus from the ZF1 direction, the characteristic binding time was in order of minutes (114±3 s, mean ± sem), as compared to the dissociation time in order of seconds (21 ± 1 s, mean ± sem; $p=0.0004$) measured when we approached the protein from the ZF3 direction. Altogether, our results suggest that a local perturbation of ZF3, either by force or by modulation of the flanking sequences proximal to it, leads to more rapid dissociation of Egr-1 from its binding site.

Discussion

We used single-molecule unzipping with optical tweezers to characterize the interactions of Egr-1 with its binding sites at the promoter of the *Lhb* gene. Measuring both the protein binding probability to the different sites and the mean force required to disrupt the bound proteins, allowed us to characterize the binding of Egr-1 at the single-molecule level. Our experiments show that the differences in sequence between these sites, and the specific genomic context where they are located, dictate different modes of interaction with the DNA. Interestingly, the breaking forces measured for the three conserved sites in the *Lhb* promoter did not correlate with their binding probability, suggesting that it is not only a modulation of the affinity of a site which is functionally important, but the specific structure of the complex, as dictated by the binding sequence and its context, is important too.

In addition, our results show that the protein-DNA complex is particularly sensitive to the properties of the DNA flanking the binding site at the side corresponding to interactions made by ZF3. Unzipping the DNA in the reverse direction, thus approaching the complex from the ZF3 side, resulted in lower breaking forces, indicating that the complex is more easily displaced if ZF3 is disrupted first. A novel method monitoring binding of Egr-1 via the reversible repression of local fluctuations in the DNA allowed us to determine that the dissociation time of Egr-1 is much shorter under a perturbation on the ZF3 side than it is under a similar perturbation on the ZF1 side, further supporting a functional role for ZF3. Interestingly, recent studies have described two possible scanning-mode

conformations(42): in the first, "scanning mode a", ZF2 and ZF3 are bound to DNA while ZF1 is not. This is the conformation originally described in Ref. (27). In the second possibility, "scanning mode b", those are ZF1 and ZF2 that interact with the DNA, while ZF3 doesn't. It is possible that the effect we observe here for the perturbation of ZF3, stems from the fact that a transition from "recognition mode" to "search mode" could be catalyzed by disrupting the interactions of either ZF1 or ZF3. Since we observe an increased sensitivity for a perturbation of ZF3, our results may suggest that "scanning mode b" is the preferred mode of scanning accessed from this binding sites.

Notably, our findings have implications for the interaction of Egr-1 with other TFs. Binding of a second TF to DNA in close proximity to the ZF3 side of a bound Egr-1 can facilitate its dissociation, thus effectively providing a mechanism of cooperativity between the TFs. Interestingly, site -2 in the *Lhb* gene is located immediately upstream of the binding site for Pitx1, and downstream from the binding site of SF-1. These three TFs have been found to act in a highly cooperatively manner in the GnRH-induced expression of *Lhb*(20, 43, 44), hence it is possible that the mechanism outlined here plays a role in modulating their interaction. Our results can also shed light on the interaction of Egr-1 with other cellular molecular motors translocating on DNA. The mammalian genome harbors $\sim 10^6$ sites that are highly similar to the classical recognition sequence of Egr-1(28). Some of these sites are *bona fide* regulatory elements, but most will likely be located at the body of genes. Previous studies have highlighted the importance of these quasi-specific sites for the kinetics of the Egr-1 finding its regulatory targets, as they can slow down the search process(30). However, binding of Egr-1 at high density on the DNA will likely affect also the function of molecular motors, e.g. polymerases, that translocate on DNA, thus potentially affecting important processes such as replication and transcription. Interestingly, while previous works have shown that many helicases are capable of displacing proteins bound to DNA (see for example Refs. (45–47)), polymerases seem to be unable to perform this task. Our results suggest a mechanism that can assist in the displacement of the quasi-specifically bound Egr-1 proteins, provided that they are in the right orientation, such that the polymerase encounters the ZF3 side first. Interestingly, all the binding sites we detected on the gene body of *Lhb* (1,2,3 in Supplementary Fig. 7) are positioned in an orientation such as an RNA polymerase transcribing the *Lhb* gene will first encounter Egr-1 from the ZF3 direction.

Finally, the approach described to study Egr-1 has the potential shed light on the interaction of other TFs with DNA. Interestingly, previous studies analyzing genomic variation in humans(48) have shown that the majority of significant genetic variants is located in non-coding regions, and that complex organismal phenotypes are the result of altered binding of TFs. However, only a small fraction of these variations in TF binding is caused by variants directly disrupting the TF recognition motif(49). Hence, a better understanding of the molecular mechanism by which flanking sequences modulate binding of TFs to DNA can shed light on inter-individual phenotypic variations and improve our ability to dissect its molecular roles in disease susceptibility.

Methods

Reagents

The original plasmid for Egr-1 (DNA binding domain) was kindly provided by Dr. Scot Wolfe. The protein was expressed and purified as previously described(50), by cloning it into a pGex2t plasmid (GE Healthcare Life Sciences) along with a cleavable glutathione S-transferase (GST) tag. Fusion protein was expressed in BL21 cells grown in LB media at 37 °C, and purified using a glutathione sepharose column (GE Healthcare Life Sciences). GST tags were cleaved via room-temperature overnight incubation with thrombin (GE Healthcare Life Sciences) and then eluted. Purified protein (stock concentration 50 μM) was aliquoted and stored at −80 °C until use. Specific binding of the purified protein to DNA was verified by EMSA with DNA oligomers containing the consensus binding site.

Optical Tweezers

Experiments were performed in a custom-made double-trap optical tweezers apparatus(51), as previously described(8, 52). Briefly, the beam from an 852 nm laser (TA PRO, Toptica) was coupled into a polarization-maintaining single-mode optical fiber. The collimated beam out of the fiber, with a waist of w_0=4mm, was split by a polarizing beam splitter (PBS) into two orthogonal polarizations, each directed into a mirror and combined again with a second BS. One of the mirrors is mounted on a nanometer scale mirror mount (Nano-MTA, Mad City Labs). A X2 telescope expands the beam, and also images the plane of the mirrors into the back focal plane of the focusing microscope objective (Nikon, Plan Apo VC 60X, NA/1.2). Two optical traps are formed at the objective's focal plane, each by a different polarization, and with a typical stiffness of 0.3-0.5 pN/nm. The light is collected by a second, identical objective, the two polarizations separated by a BS, and imaged onto two Position Sensitive Detectors (First Sensor). The position of the beads relative to the center of the trap is determined by back focal plane interferometry(53). Calibration of the setup was done by analysis of the thermal fluctuations of the trapped beads(54), which were sampled at 100kHz.

Molecular construct for single molecule experiments

The constructs for single-molecule experiments were generated as described previously(8), with a number of modification. Briefly, TF binding DNA segments with the *Lhb* promoter sequence were amplified by PCR from mouse genomic DNA, and segments for the non-native context (C1 and C2) were amplified from a plasmid containing the 601 nucleosome positioning sequence(55), a generous gift from Daniela Rhodes (MRC, Cambridge, UK). Primers used for the amplification reactions are listed in Supplementary Tables 9-10. For forward unzipping experiments, the constructs were digested using DraIII-HF (New England Biolabs) overnight according to the manufacturer's instructions. A 10 bp hairpin (Sigma) was ligated to the construct using T4 DNA ligase (New England Biolabs), in a reaction with 1:10 molar excess of the hairpin, at 16 °C. The construct was subsequently digested overnight with BglI (New England Biolabs). For reverse unzipping the constructs were digested using BglI, hairpin-ligated and subsequently digested overnight with

DraIII-HF. We generated two ~2000-bp DNA handles, each incorporating a specific tag (double digoxygenin and biotin), using commercially purchased 5' modified primers in a standard PCR reaction, using bacteriophage lambda DNA as a template. The other two primers were designed to contain repeats of three DNA sequences recognized by single strand nicking enzymes: Nt.BbvCI and Nb.BbvCI (both from New England Biolabs) on the biotin-tagged handle and on the digoxygenin-tagged handle, respectively. The nicking enzymes generated 29 nt complementary overhangs on each handle. Handles were mixed at equal molar ratios for DNA annealing, creating a ~4000 bp fragment of annealed DNA handles. A ~350 bp dsDNA alignment segment with the sequence of the 601 DNA was prepared using commercially purchased primers (Supplementary Table 11) in a standard PCR reaction, ligated to the handles, and gel-purified (QIAquick 28706, Qiagen). Binding segments were ligated to DNA handles using a rapid ligase system (Promega) in 3:1 molar ratio, 30 min at room temp. The full construct (i.e. handles + alignement segment + TF binding segment) was incubated for 15 min on ice with 0.8 μm polystyrene beads (Spherotech), coated with anti-Digoxigenin (anti-DIG). The reaction was then diluted 1000-fold in binding buffer (10 mM Tris·Cl pH 7.4, 1 mM EDTA, 150 mM NaCl, 1.5 mM $MgCl_2$, 1 mM DTT, 3% v/v glycerol and 0.01% BSA). Tether formation was performed *in situ* (inside the experimental chamber) by trapping an anti-DIG bead (bound by nucleosomes) in one trap, trapping a 0.9 μm streptavidin coated polystyrene beads in the second trap, and bringing the two beads into close proximity to allow binding of the biotin tag in the nucleosomal DNA to the streptavidin in the bead.

Data analysis

Data were digitized at a sampling rate fs=2500 Hz, and saved to a disk. All further processing of the data was done with Matlab (Mathworks). Stretching of the tether was used to find the polymer-models parameters under our experimental conditions. Stretching to 15 pN was used to fit an extensible worm-like-chain model (XWLC) for the stretching of the dsDNA handles, and the data at forces above the unzipping of DNA was used to fit a worm-like-chain (WLC) model for the released ssDNA. From the measured and filtered tether extension and force, the stretching of the dsDNA handles at each time point was subtracted from the measured extension. Then, the extension was divided by the extension of two ssDNA bases (calculated from the measured force using the WLC model) to result in the number of unzipped bp. To improve the accuracy of the experiments, a ~250 bp naked DNA alignment segment was ligated prior to the binding segment (56). This segment was used to perform a correlation-based alignment of all traces in a group (i.e. DNA sequence) to a single curve used as a master curve, allowing shifting of the traces (i.e. redefining the position of zero extension) and stretching of up to 2%. Binding events were identified by detecting an increase in force of more than 0.5pN as compared to the median force at the same position, for experiments with the same DNA construct but in the absence of Egr-1. Applying the same criteria for the data obtained without Egr-1 resulted in no binding events detected. Events were classified as belonging to a specific site if the breaking event was located within a 20 bp window relative to the expected center of the binding site. Differences in breaking forces were checked

using a two-tail Student's t-test. Differences in binding probability were checked using a Chi-squared test. Differences were considered statistically significant if the calculated p-value was no larger than 0.05.

Dissociation time measurements

DNA was unzipped until reaching an extension corresponding to the Egr-1 consensus binding site. The position of the unzipping fork was further adjusted to a mean extension and force that results in equal mean residency times between a locally 'closed' (dsDNA) and 'open' (ssDNA) configuration of the consensus DNA. The fluctuations in extension over time were measured for 1 min before the exposure to Egr-1, after which the construct was moved to a region of the laminar flow chamber that contains Egr-1. Binding of the protein was detected by a sudden transition to a 'closed' state and a prolonged residence time in this configuration. No binding events were detected in the absence of protein (Supplementary Fig. 8a). The dissociation time was taken as the time lapsed until the reappearance of the fluctuations. Two different methods were used: In the first, following binding the construct was moved back to the channel in which Egr-1 was absent, to prevent re-binding, thus providing a single event of dissociation. In the second (Supplementary Fig. 8c) multiple binding and dissociation events were observed by keeping the construct at the Egr-1 channel.

Acknowledgements

We acknowledge support from the Israel Science Foundation (Grant 1782/17 to AK), the Israeli Centers of Research Excellence program (I-CORE, Center no. 1902/12 to A.K), the European Commission (Grant 293923 to AK), and the Eliyahu Pen Research Fund.

Author Contributions

S.R. and H.K. performed the experiments. O.M. and A.K. designed and built the optical tweezers setup. S.R., H.K. and A.K. analyzed the data. A.S. and A.M. prepared reagents. S.R. and A.K. wrote the paper. P.M. and A.K supervised the research.

References

1. Weirauch MT, et al. (2014) Determination and Inference of Eukaryotic Transcription Factor Sequence Specificity. *Cell* 158(6):1431–1443.
2. Nitta KR, et al. (2015) Conservation of transcription factor binding specificities across 600 million years of bilateria evolution. *Elife* 4. doi:10.7554/eLife.04837.
3. Jolma A, et al. (2013) DNA-Binding Specificities of Human Transcription Factors. *Cell* 152(1–2):327–339.
4. Rohs R, et al. (2009) The role of DNA shape in protein–DNA recognition. *Nature* 461(7268):1248–1253.
5. Yang L, et al. (2014) TFBSshape: a motif database for DNA shape features of transcription factor binding sites. *Nucleic Acids Res* 42(D1):D148–D155.
6. Polach KJ, Widom J (1995) Mechanism of protein access to specific DNA sequences in chromatin: a dynamic equilibrium model for gene regulation. *J Mol Biol* 254(2):130–49.
7. Raveh-Sadka T, Levo M, Segal E (2009) Incorporating nucleosomes into thermodynamic models of transcription regulation. *Genome Res* 19(8):1480–96.
8. Rudnizky S, et al. (2016) H2A.Z controls the stability and mobility of nucleosomes to regulate expression of the LH genes. *Nat Commun* 7:12958.
9. Meijsing SH, et al. (2009) DNA Binding Site Sequence Directs Glucocorticoid Receptor Structure and Activity. *Science (80-)* 324(5925):407–410.
10. Panne D (2008) The enhanceosome. *Curr Opin Struct Biol* 18(2):236–242.
11. Wasson T, Hartemink AJ (2009) An ensemble model of competitive multi-factor binding of the genome. *Genome Res* 19(11):2101–12.
12. Kitayner M, et al. (2010) Diversity in DNA recognition by p53 revealed by crystal structures with Hoogsteen base pairs. *Nat Struct Mol Biol* 17(4):423–429.
13. Mirny LA (2010) Nucleosome-mediated cooperativity between transcription factors. *Proc Natl Acad Sci U S A* 107(52):22534–9.
14. Mirny L, et al. (2009) How a protein searches for its site on DNA: the mechanism of facilitated diffusion. *J Phys A Math Theor* 42(43):434013.
15. Kolomeisky AB (2011) Physics of protein-DNA interactions: mechanisms of facilitated target search. *Phys Chem Chem Phys* 13(6):2088–95.
16. Lazarovici A, et al. (2013) Probing DNA shape and methylation state on a genomic scale with DNase I. *Proc Natl Acad Sci* 110(16):6376–6381.
17. Fahmy RG, Dass CR, Sun L-Q, Chesterman CN, Khachigian LM (2003) Transcription factor Egr-1 supports FGF-dependent angiogenesis during neovascularization and tumor growth. *Nat Med* 9(8):1026–1032.
18. Jouvert P, et al. (2004) Activation of the cGMP Pathway in Dopaminergic Structures Reduces Cocaine-Induced EGR-1 Expression and Locomotor Activity. *J Neurosci* 24(47):10716–10725.
19. Sayasith K, Brown KA, Lussier JG, Dore M, Sirois J (2006) Characterization of bovine

early growth response factor-1 and its gonadotropin-dependent regulation in ovarian follicles prior to ovulation. *J Mol Endocrinol* 37(2):239–250.

20. Tremblay JJ, Drouin J (1999) Egr-1 is a downstream effector of GnRH and synergizes by direct interaction with Ptx1 and SF-1 to enhance luteinizing hormone beta gene transcription. *Mol Cell Biol* 19(4):2567–76.

21. Wong DL, Tai TC, Wong-Faull DC, Claycomb R, Kvetnansky R (2004) Genetic mechanisms for adrenergic control during stress. *Annals of the New York Academy of Sciences* doi:10.1196/annals.1296.048.

22. Christy B, Nathans D (1989) DNA binding site of the growth factor-inducible protein Zif268. *Biochemistry* 86:8737–8741.

23. Pavletich NNP, Pabo COC 0 (1991) Zinc finger-DNA recognition: crystal structure of a Zif268-DNA complex at 2.1 A. *Science (80-)* 252(5007):809–17.

24. Yan S-F, et al. (2000) Egr-1, a master switch coordinating upregulation of divergent gene families underlying ischemic stress. *Nat Med* 6(12):1355–1361.

25. Khachigian LM, Lindner V, Williams AJ, Collins T (1996) Egr-1-induced endothelial gene expression: a common theme in vascular injury. *Science* 271(5254):1427–31.

26. Slutsky M, Mirny LA (2004) Kinetics of Protein-DNA Interaction: Facilitated Target Location in Sequence-Dependent Potential. *Biophys J* 87(6):4021–4035.

27. Zandarashvili L, et al. (2012) Asymmetrical roles of zinc fingers in dynamic DNA-scanning process by the inducible transcription factor Egr-1. *Proc Natl Acad Sci* 109(26):E1724–E1732.

28. Kemme CA, Esadze A, Iwahara J (2015) Influence of quasi-specific sites on kinetics of target DNA search by a sequence-specific DNA-binding protein. *Biochemistry* 54(44):6684–91.

29. Chattopadhyay A, Zandarashvili L, Luu RH, Iwahara J (2016) Thermodynamic Additivity for Impacts of Base-Pair Substitutions on Association of the Egr-1 Zinc-Finger Protein with DNA. *Biochemistry* 55(47):6467–6474.

30. Kemme CA, Esadze A, Iwahara J (2015) Influence of Quasi-Specific Sites on Kinetics of Target DNA Search by a Sequence-Specific DNA-Binding Protein. *Biochemistry* 54(44):6684–6691.

31. Chattopadhyay A, Zandarashvili L, Luu RH, Iwahara J (2016) Thermodynamic Additivity for Impacts of Base-Pair Substitutions on Association of the Egr-1 Zinc-Finger Protein with DNA. *Biochemistry* 55(47):6467–6474.

32. Lee SL, et al. (1996) Luteinizing hormone deficiency and female infertility in mice lacking the transcription factor NGFI-A (Egr-1). *Science* 273(5279):1219–21.

33. Koch SJ, Wang MD (2003) Dynamic Force Spectroscopy of Protein-DNA Interactions by Unzipping DNA. *Phys Rev Lett* 91(2):28103.

34. Koch SJ, Shundrovsky A, Jantzen BC, Wang MD (2002) Probing Protein-DNA Interactions by Unzipping a Single DNA Double Helix. *Biophys J* 83(2):1098–1105.

35. Jiang J, et al. (2005) Detection of High-Affinity and Sliding Clamp Modes for MSH2-MSH6 by Single-Molecule Unzipping Force Analysis. *Mol Cell* 20(5):771–781.

36. Li M, et al. (2015) Dynamic regulation of transcription factors by nucleosome

remodeling. *Elife* 4:e06249.

37. Call GB, Wolfe MW (2002) Species differences in GnRH activation of the LHβ promoter: role of Egr1 and Sp1. *Mol Cell Endocrinol* 189(1–2):85–96.

38. Elrod-Erickson M, Rould MA, Nekludova L, Pabo CO (1996) Zif268 protein-DNA complex refined at 1.6 A: a model system for understanding zinc finger-DNA interactions. *Structure* 4(10):1171–80.

39. Schöne S, et al. (2016) Sequences flanking the core-binding site modulate glucocorticoid receptor structure and activity. *Nat Commun* 7:12621.

40. Levo M, et al. (2015) Unraveling determinants of transcription factor binding outside the core binding site. *Genome Res* 25(7):1018–29.

41. Dror I, Golan T, Levy C, Rohs R, Mandel-Gutfreund Y (2015) A widespread role of the motif environment in transcription factor binding across diverse protein families. *Genome Res* 25(9):1268–80.

42. Zandarashvili L, et al. (2015) Balancing between affinity and speed in target DNA search by zinc-finger proteins via modulation of dynamic conformational ensemble. *Proc Natl Acad Sci U S A* 112(37):E5142–E5149.

43. Dorn C, Ou Q, Svaren J, Crawford PA, Sadovsky Y (1999) Activation of luteinizing hormone beta gene by gonadotropin-releasing hormone requires the synergy of early growth response-1 and steroidogenic factor-1. *J Biol Chem* 274(20):13870–6.

44. Halvorson LM, Kaiser UB, Chin WW (1999) The Protein Kinase C System Acts through the Early Growth Response Protein 1 to Increase LHβ Gene Expression in Synergy with Steroidogenic Factor-1. *Mol Endocrinol* 13(1):106–116.

45. Mackintosh SG, Raney KD (2006) DNA unwinding and protein displacement by superfamily 1 and superfamily 2 helicases. *Nucleic Acids Res* 34(15):4154–9.

46. Byrd AK, Raney KD (2006) Displacement of a DNA binding protein by Dda helicase. *Nucleic Acids Res* 34(10):3020–3029.

47. Finkelstein IJ, Visnapuu M-L, Greene EC (2010) Single-molecule imaging reveals mechanisms of protein disruption by a DNA translocase. *Nature* 468(7326):983–987.

48. Auton A, et al. (2015) A global reference for human genetic variation. *Nature* 526:68–74.

49. Deplancke B, Alpern D, Gardeux V (2016) The Genetics of Transcription Factor DNA Binding Variation. *Cell* 166:538–554.

50. Squires A, et al. (2015) Nanopore sensing of individual transcription factors bound to DNA. *Sci Rep* 5(1):11643.

51. Moffitt JR, Chemla YR, Izhaky D, Bustamante C (2006) Differential detection of dual traps improves the spatial resolution of optical tweezers. *Proc Natl Acad Sci U S A* 103(24):9006–11.

52. Malik O, Khamis H, Rudnizky S, Marx A, Kaplan A (2017) Pausing kinetics dominates strand-displacement polymerization by reverse transcriptase. *Nucleic Acids Res* 42:434011.

53. Gittes F, Schmidt CF (1998) Interference model for back-focal-plane displacement detection in optical tweezers. *Opt Lett* 23(1):7–9.

54. Berg-Sørensen K, Flyvbjerg H, Introduction I, Berg-Sørensen K, Flyvbjerg H (2004) Power spectrum analysis for optical tweezers. *Rev Sci Instrum* 75(3):594–612.

55. Lowary P. T, Widom J (1998) New DNA sequence rules for high affinity binding to histone octamer and sequence-directed nucleosome positioning. *J Mol Biol* 276(1):19–42.

56. Killian JL, Li M, Sheinin MY, Wang MD (2012) Recent advances in single molecule studies of nucleosomes. *Curr Opin Struct Biol* 22(1):80–7.

Figures

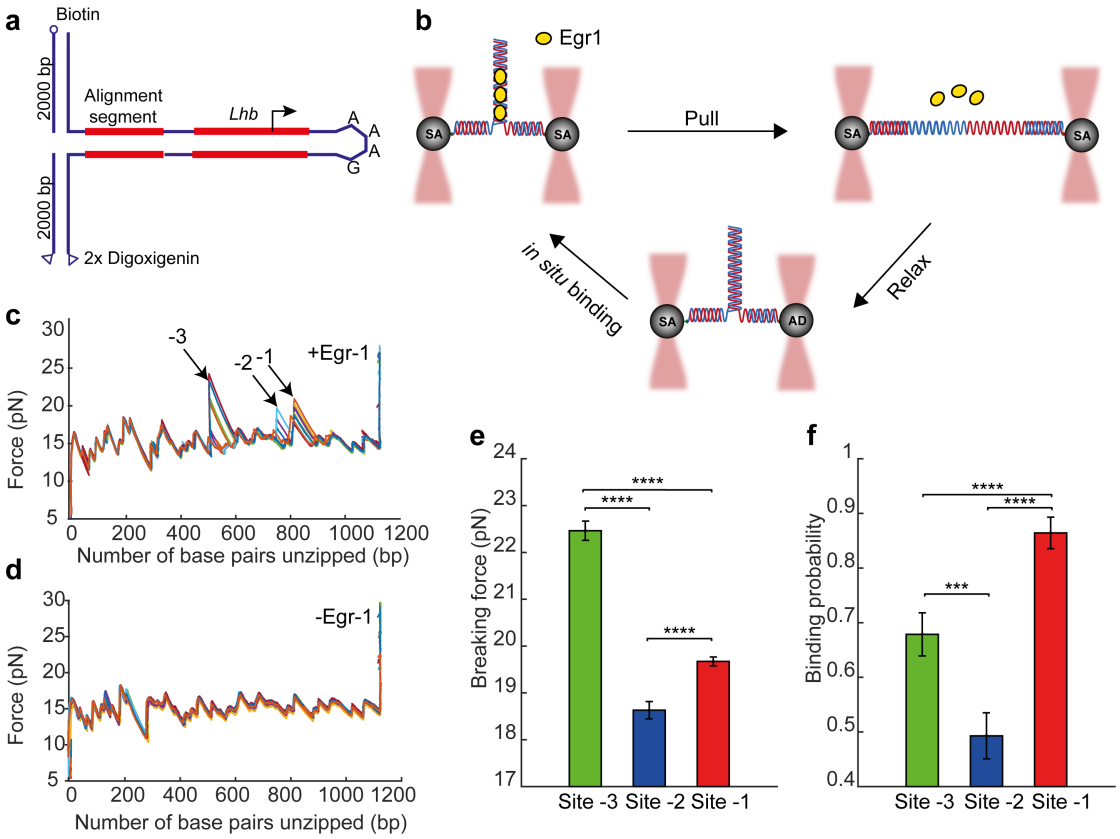

Figure 1: Single-molecule probing of Egr-1 binding to the *Lhb* promoter. a) The -517/+246 of mouse *Lhb* DNA is ligated to a fixed 345 bp alignment sequence and a short stem-loop that prevents breaking of the tether after unzipping. b) The *Lhb* DNA is connected to two 2kb dsDNA molecular handles, which are attached to polystyrene beads trapped in two separate optical traps. Egr-1 binding to the construct is initiated *in situ* (inside experimental chamber). One of the traps is moved to stretch the tethered construct and disrupt protein-DNA interactions. After unzipping the whole construct, the DNA us relaxed and dsDNA forms again. The process is repeated multiple times. c-d) Unzipping force-extension curves of *Lhb* in the presence (c) and absence (d) of Egr-1. Egr-1 binding to each of the sites (-1/-2/-3) is designate with arrows. e) Breaking force for three Egr-1 binding sites located on the *Lhb* promoter. Data shown as mean±s.e.m., n=140; ****p<0.0001, two-sample Student's T-test. f) Binding probability, calculated as the number of binding events out of the total number of DNA unzipping cycles, for each of the three Egr-1 binding sites at [Egr-1]=500 nM. Data shown as fraction±s.e., n=140; ****p<0.0001, Chi-square test.

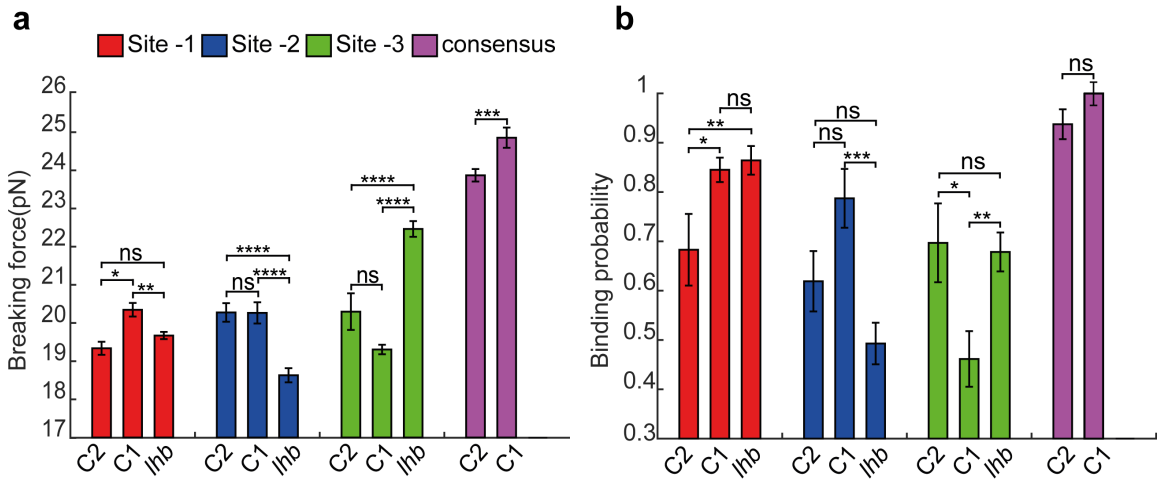

Figure 2: DNA sequence flanking the binding sites modulate Egr-1 binding. Three Egr-1 binding sites were integrated separately into a C1 and C2 DNA context (Supplementary Fig. 3) and subjected to multiple unzipping analysis in presence of 500 nM Egr-1. a) Binding probability and b) mean breaking force is presented for sites -3/-2/-1 and the consensus motif. The data is analyzed as in Fig 1. The number of experiments for each case is shown in Supplementary Table 1, and the p-values in Supplementary Table 5.

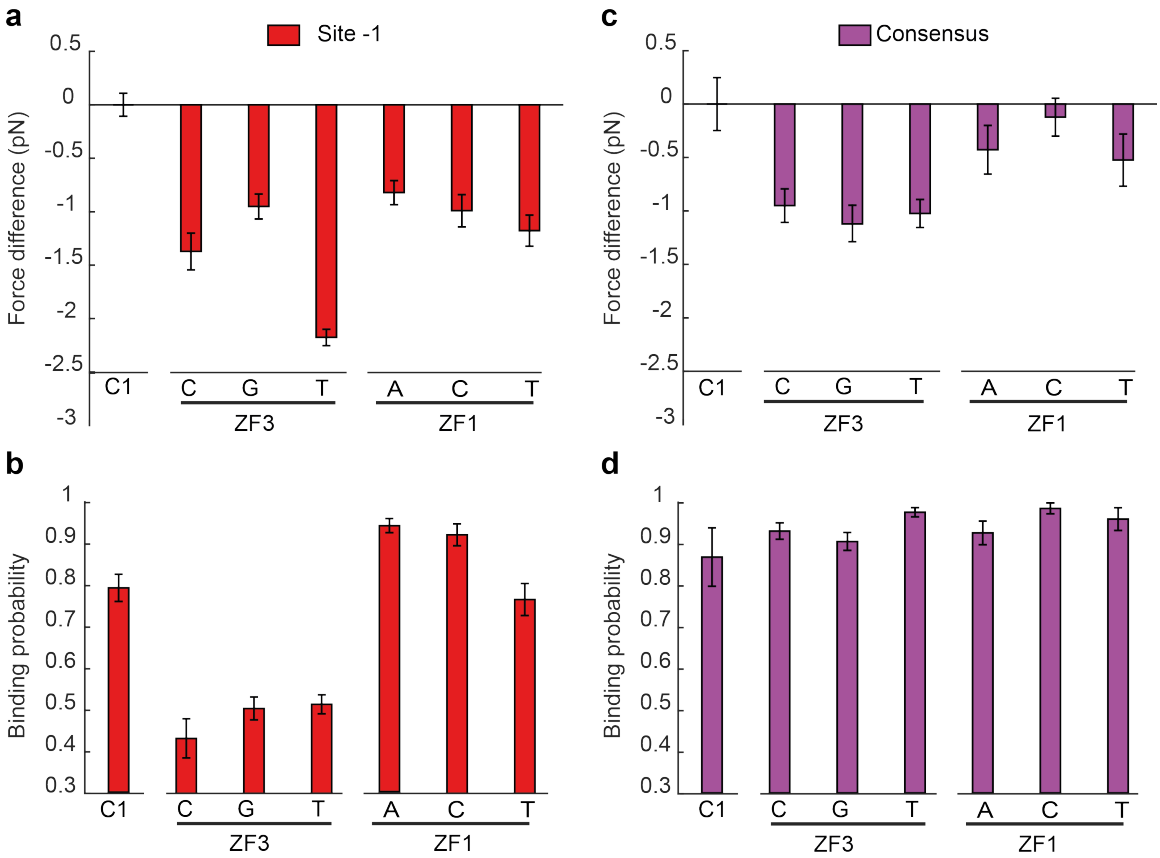

Figure 3: The first nucleotide proximal to ZF3 modulates Egr-1 binding. The first nucleotide proximal to ZF3 or to ZF1, for site -1 or the consensus sequence, both in a C1 context, was mutated for the designated nucleotides and subjected to multiple unzipping analysis in presence of 500 nM Egr-1. The data for binding probability and breaking force is analyzed and presented as in Fig 1. The number of experiments for each case is shown in Supplementary Table 2, and the p-values in Supplementary Table 6.

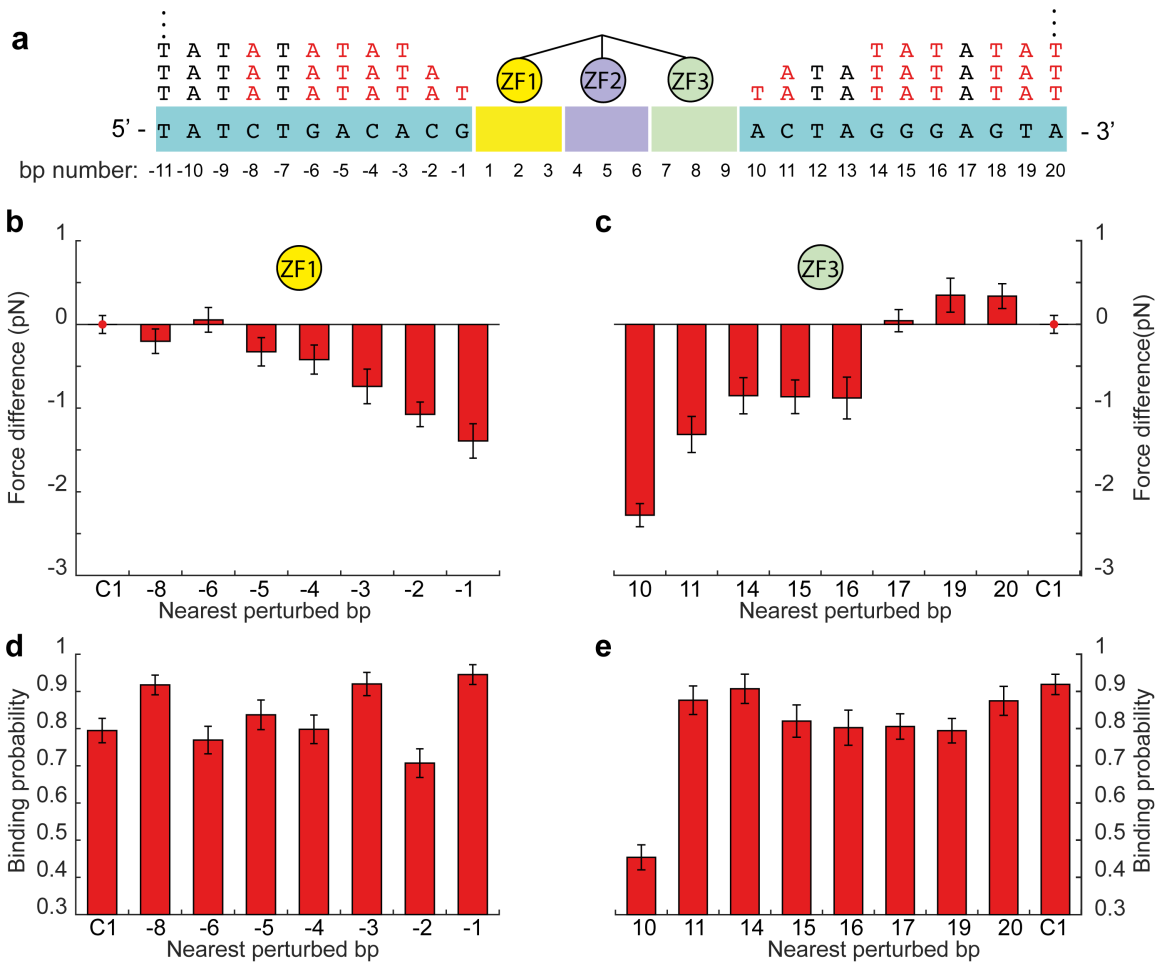

Figure 4: Effect for a gradual change of flanking context on Egr-1 binding. (a) The identity of 8-11 nucleotides proximal to ZF3 or to ZF1, for site -1 in a C1 DNA context, was gradually changed by their conversion to AT repeats. (b-e) Mutated DNA constructs of site -1 were subjected to multiple unzipping analysis in presence of 500 nM Egr-1. (b-c) Difference between the breaking force measured for the unmodified C1 context, and constructs in which nucleotides proximal to ZF1 (b) or ZF3 (c) were mutated. (d-e) The corresponding binding probabilities, analyzed and presented as in Fig 1. The number of experiments for each case is shown in Supplementary Table 3, and the p-values in Supplementary Table 7.

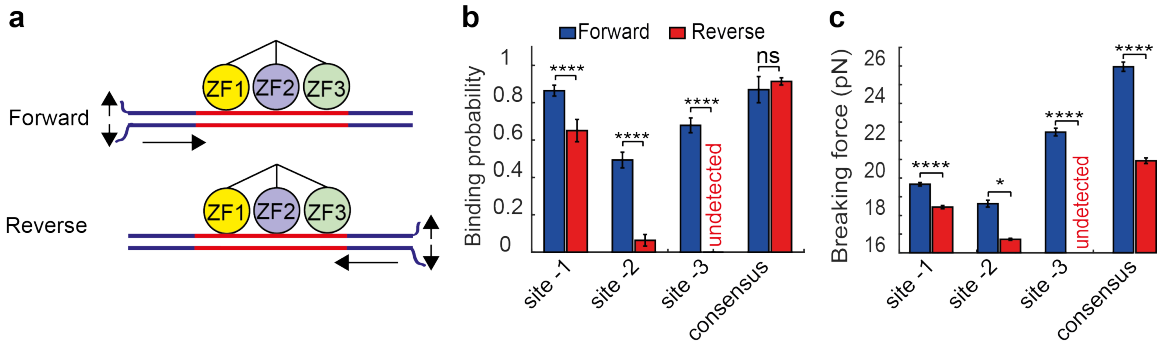

Figure 5: Unzipping Egr-1 from ZF3 direction requires less force (a) Schematic representation of forward and reverse unzipping. *Lhb* promoter or consensus motif in the C1 DNA context, were subjected to multiple repeats of forward (blue) or reverse (red) unzipping in the presence of 500 nM Egr-1. The data for binding probability (b) and breaking force (c) is analyzed and presented as in Fig. 1. The number of experiments for each case is shown in Supplementary Table 1, and the p-values in Supplementary Table 5.

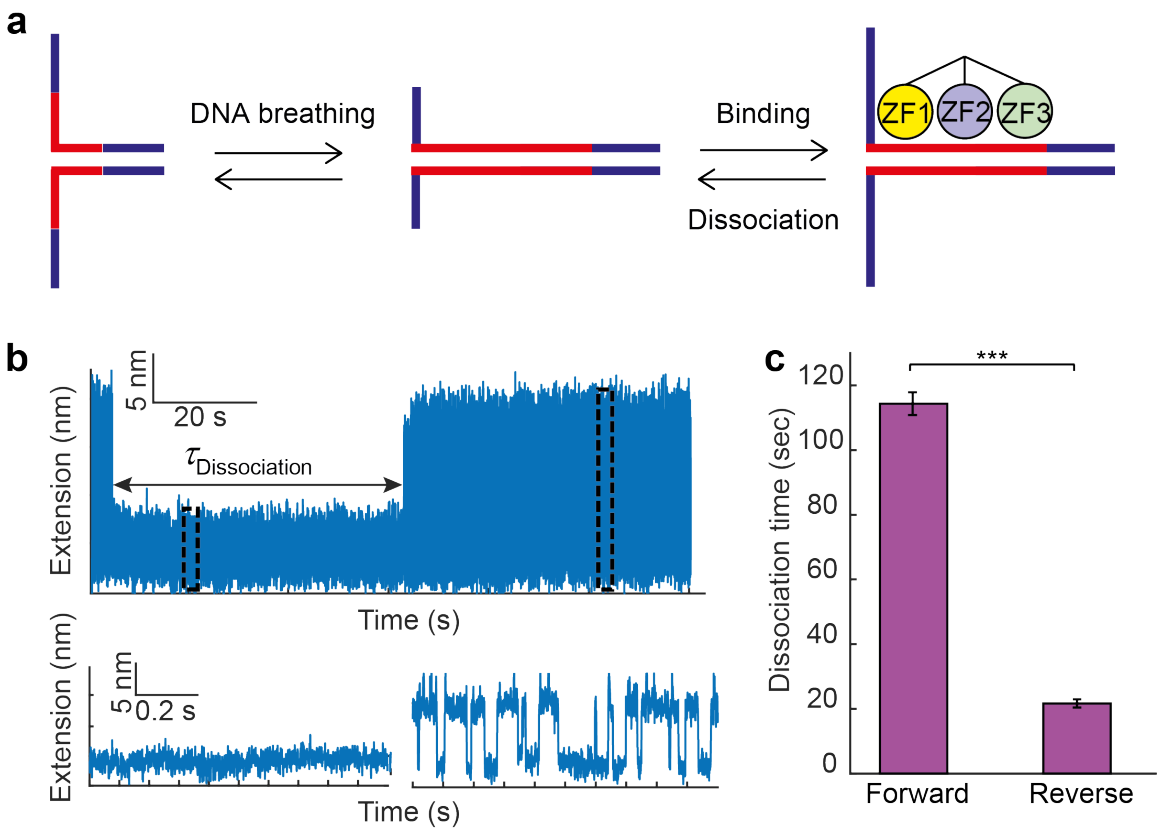

Figure 6: Force disruption of ZF3 increases Egr-1 dissociation. (a) A single-molecule containing a consensus motif (red) in the C1 context was unzipped until the fork reached the binding site. (b) The construct is held under tension, letting the DNA fluctuate between locally 'open' and 'closed' states. Binding of Egr-1 to the DNA stabilizes the closed conformation, leading to a sudden repression of the fluctuations, which lasts until Egr-1 dissociation. The time difference between binding and unbinding (dissociation time) was measured for forward (disruption of ZF1) and reverse (disruption of ZF3) unzipping. c) Mean dissociation time, calculated for forward and reverse unzipping. Data shown as mean±s.e.m., n=25 and 14. ***$p<0.001$, two-sample Student's T-test.

Supplementary Information

Single-molecule DNA unzipping reveals asymmetric modulation of the transcription factor Egr-1 by its binding site sequence and context

Sergei Rudnizky[1,2,*], Hadeel Khamis[1,3,*], Omri Malik[1,2], Allison Squires[4], Amit Meller[2,4,5], Philippa Melamed[1,2] and Ariel Kaplan[1,2,#]

[1]Faculty of Biology, Technion – Israel Institute of Technology, Haifa (32000), Israel

[2]Russell Berrie Nanotechnology Institute, Technion – Israel Institute of Technology, Haifa (32000), Israel

[3]Faculty of Physics, Technion – Israel Institute of Technology, Haifa (32000), Israel

[4]Department of Biomedical Engineering, Boston University, Boston, MA 02215, USA

[5]Faculty of Biomedical Engineering, Technion – Israel Institute of Technology, Haifa (32000), Israel

* These authors contributed equally to this work
#To whom correspondence should be addressed;
email: akaplanz@technion.ac.il

Supplementary Figures

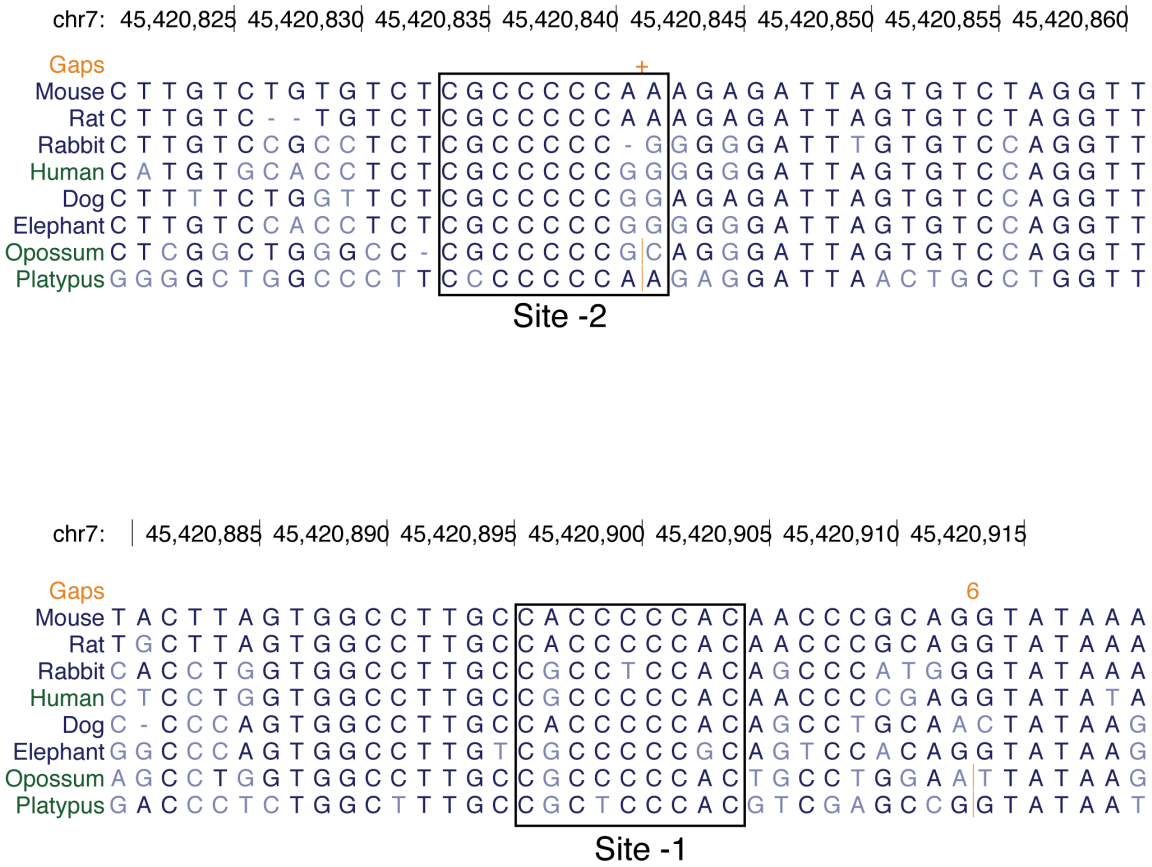

Supplementary Figure 1: Binding sites for Egr-1 at the promoter of *Lhb* are evolutionary conserved. Alignment of the proximal *Lhb* promoters from different species. Bases are numbered relative to the transcriptional start site (+1; not shown). The conserved Egr-1 response elements are boxed. Nucleotides that differ between the species are shaded. The data was generated with the Genome Browser software, http://genome.ucsc.edu/.

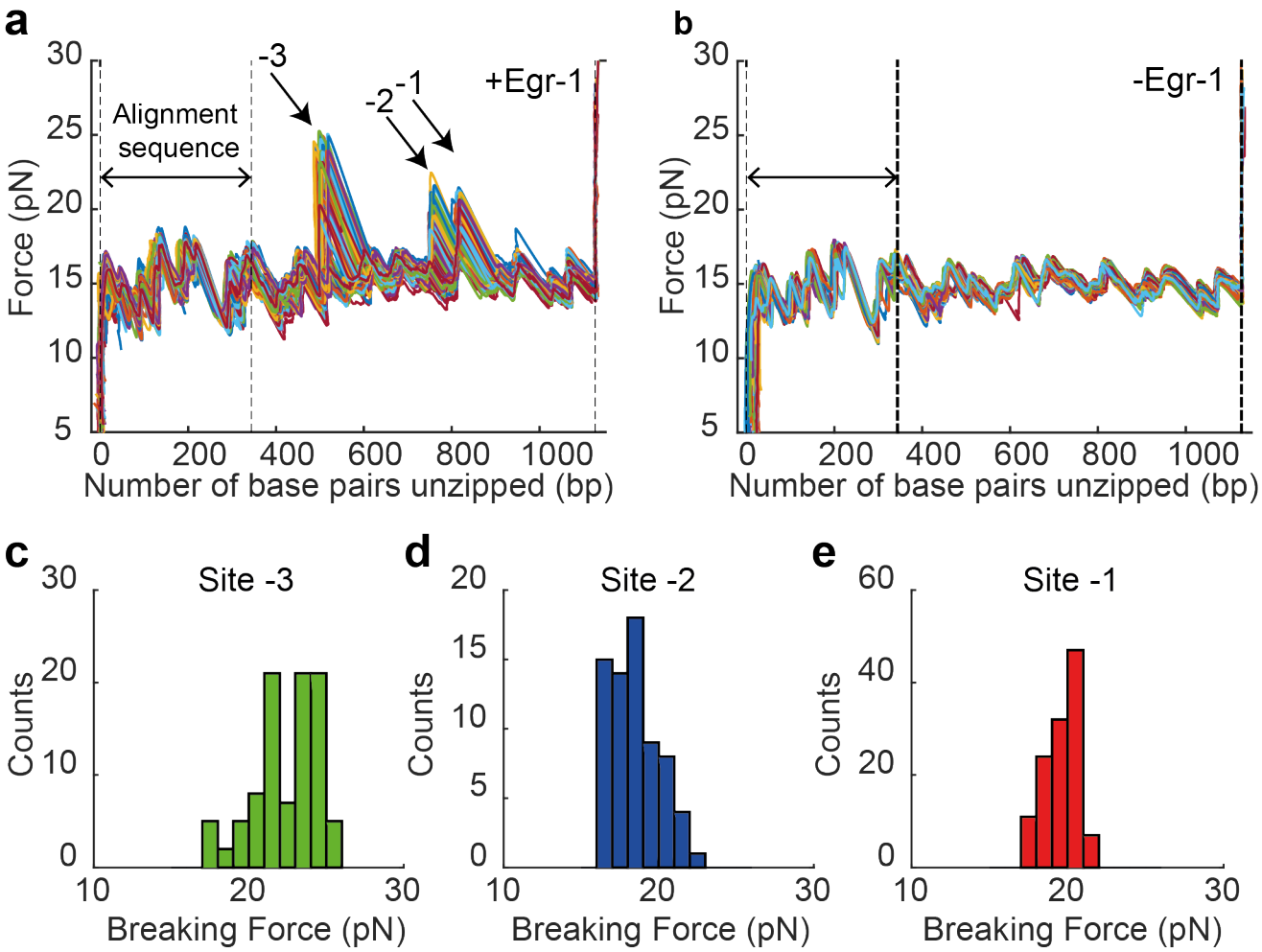

Supplementary Figure 2: Characterization of binding probability and breaking force for sites -1,-2 and -3 in *Lhb*. (a-b) All the collected traces for forward unzipping of *Lhb* in the presence (a) and absence (b) of Egr-1 (n=140 and 48, respectively). (c-d) Histograms for the breaking force for sites -3 (c), -2 (d) and -1 (d).

lhb site -3	....5'-G	C	A	A	A	T	T	T	G	G	A	[ggcccactc]	G	T	C	A	G	A	A	C	C	T	A-3'...
lhb site -2	....5'-T	G	T	C	T	G	T	G	T	C	T	[cgcccccaa]	A	G	A	G	A	T	T	A	G	T	G-3'...
lhb site -1	....5'-A	G	T	G	G	C	C	T	T	G	C	[cacccccac]	A	A	C	C	C	G	C	A	G	G	T-3'...
C1	....5'-T	A	T	C	T	G	A	C	A	C	G	[Binding site]	A	C	T	A	G	G	G	A	G	T	A-3'...
C2	....5'-T	C	A	C	T	G	C	C	G	G	C	[Binding site]	G	A	T	G	T	A	T	A	T	A	T-3'...

Supplementary Figure 3: DNA context surrounding the 9 bp core binding sites probed in the multiple unzipping experiments. 11 base pairs surrounding the naturally occurring sites on *Lhb* promoter (*Lhb* site -1/-2/-3) or supplied by the C1 or C2 contexts where the core binding sites were integrated.

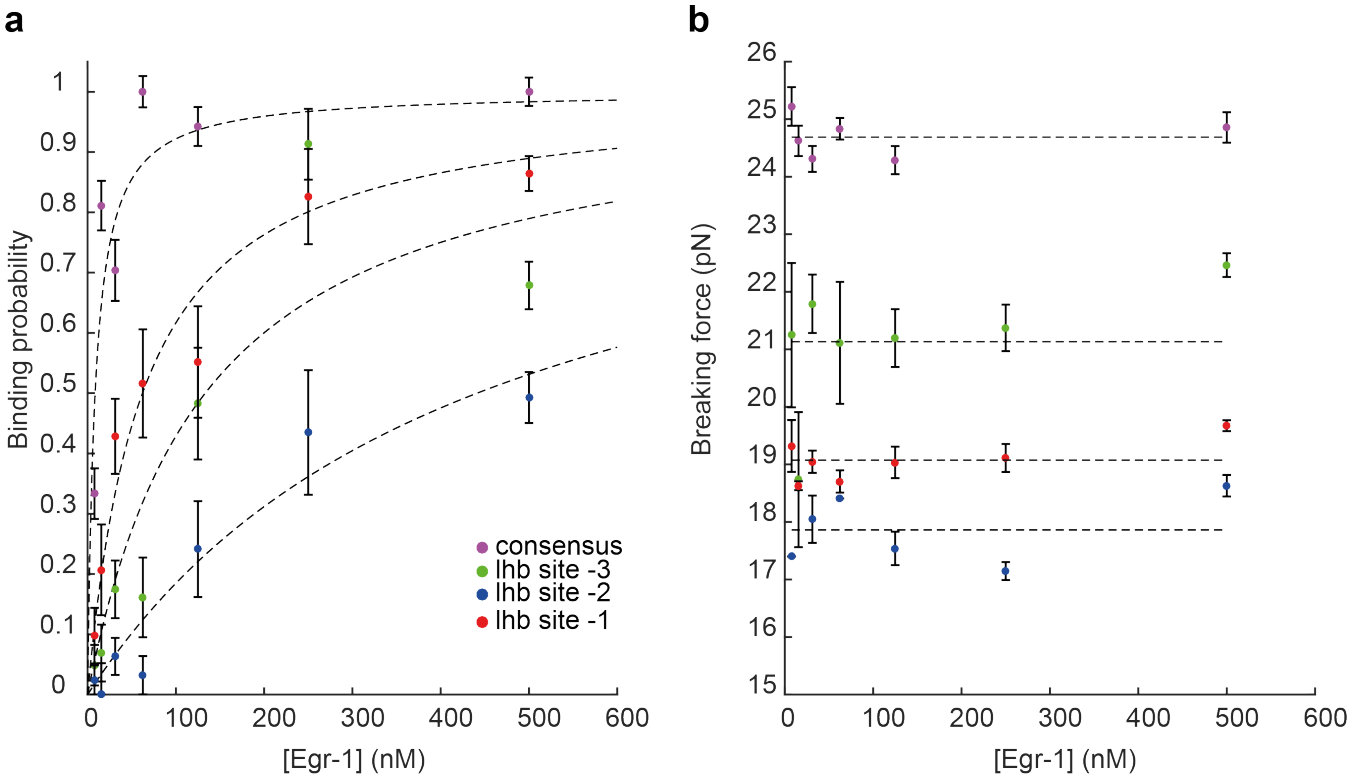

Supplementary Figure 4: The binding probability depends on [Egr-1], but the breaking force is concentration independent. Multiple unzipping experiments were performed for *Lhb* and for the consensus sequence integrated into the C1 DNA context, as a function of the concentration of Egr-1. a) The binding probability and b) mean breaking force data presented for sites -3/-2/-1 and consensus. The data is analyzed as in Fig 1. The dashed lines are hyperbolic (a) and linear (b) fits. The number of events for each case is shown in Supplementary Table 4.

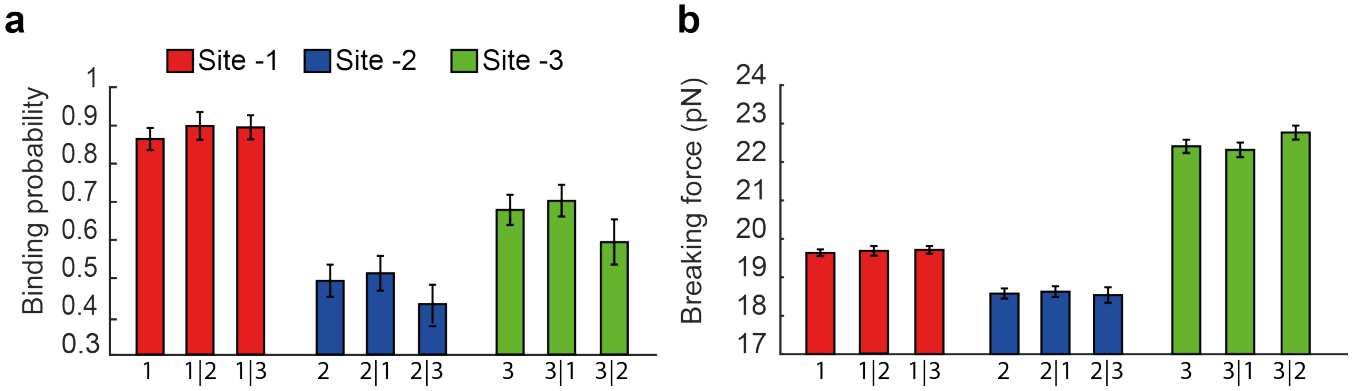

Supplementary Figure 5: Binding of Egr-1 to a given site is independent of the occupancy of other sites *in cis*. Binding probabilities (a) and mean breaking force (b) are shown for sites -1, -2 and -3 on *Lhb* DNA, both for the complete data set as well as for the conditional subsets (*r*|*s* indicates binding to site *r*, provided that site *s* was bound too). The data is analyzed and presented as in Fig 1. *n*=140.

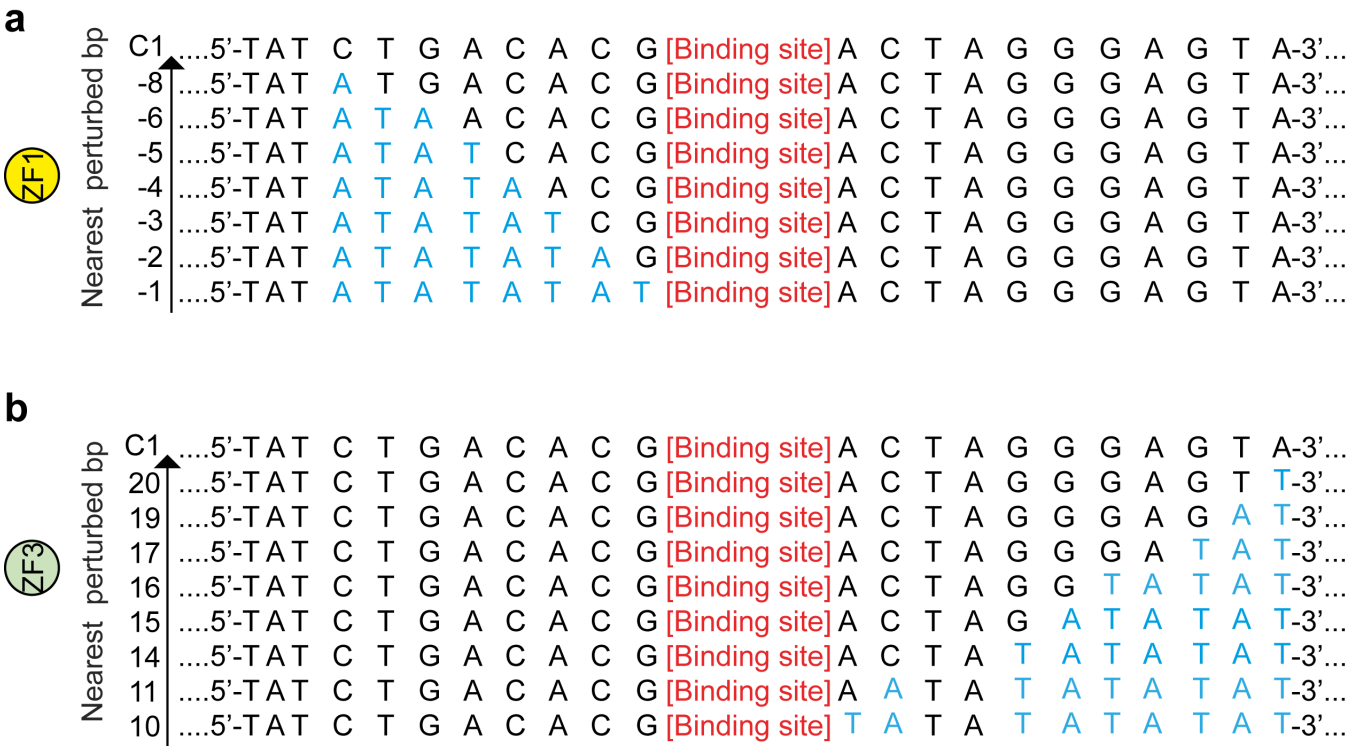

Supplementary Figure 6: Constructs used to characterize the extent of the flanking sequence effect. (a-b) Constructs used to perturb the flanking sequence at the ZF1 (a) or ZF3 (b) side of the core binding site. Mutagenized bases are shown in blue.

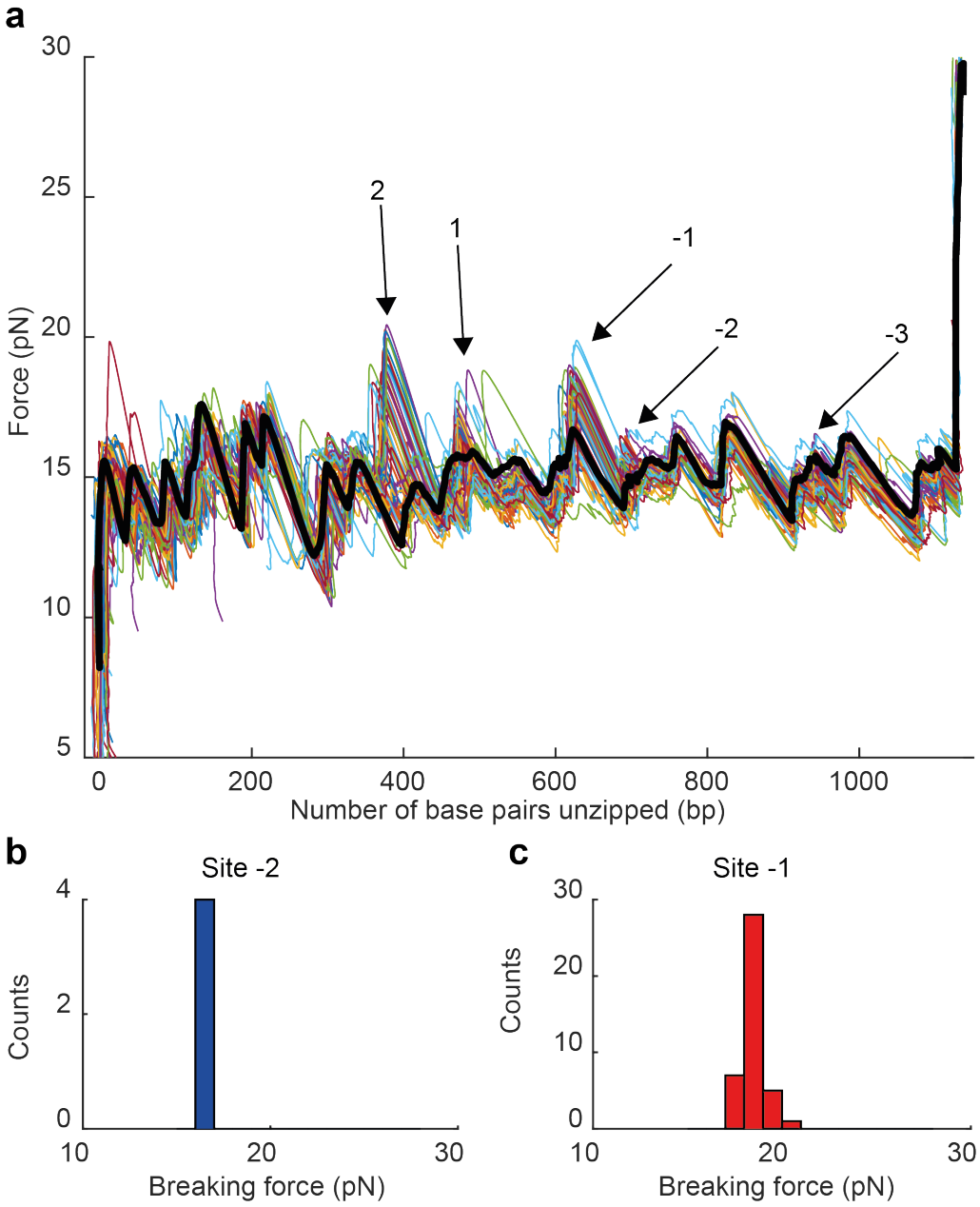

Supplementary Figure 7: Characterization of binding probability and breaking force by reverse-unzipping *Lhb*. (a) All the collected traces for reverse unzipping of *Lhb* in the presence of Egr-1 (n = 63). The position of sites -1, -2 and -3 is indicated. Sites 1 and 2, located in the gene body, were only observed in reverse unzipping. A representative trace in the absence of Egr-1 is shown in black. (b) Histograms for the breaking force for sites -2 and -1.

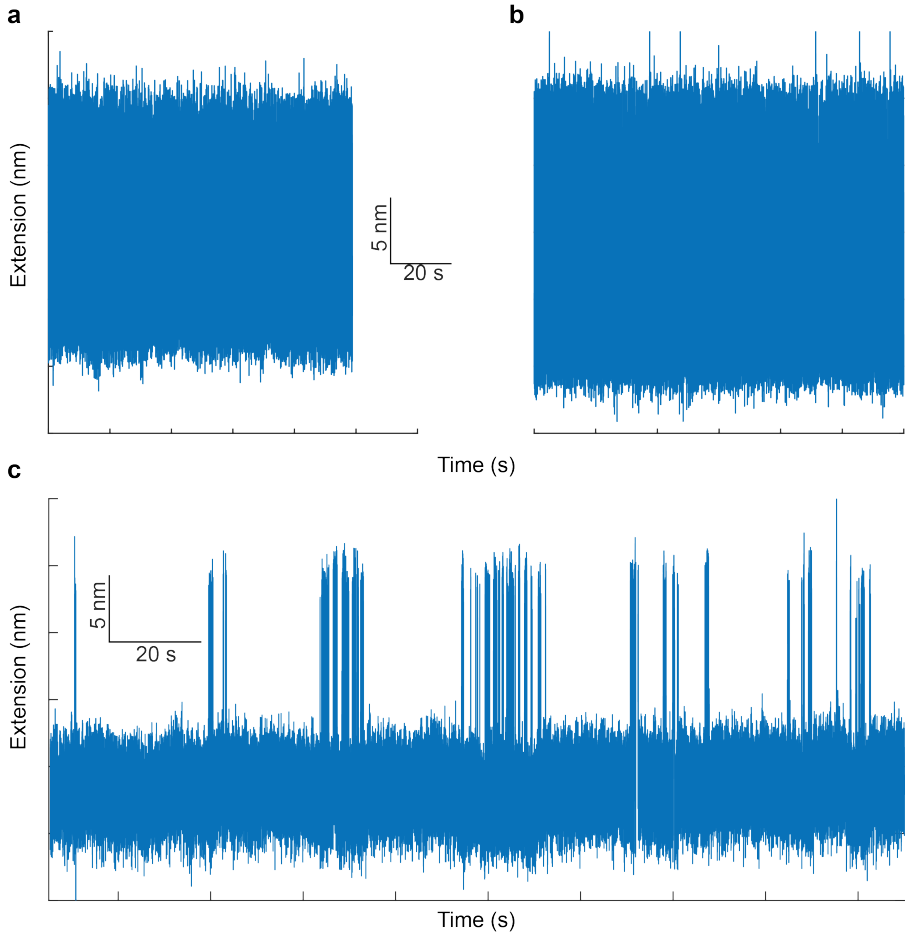

Supplementary Figure 8: Dissociation time measurements. (a) No suppression of fluctuations is observed in the absence of Egr-1, both for forward (a) and reverse (b) unzipping. (c) Multiple events of binding and dissociation are observed if the construct is kept at the Egr-1 flow channel. Data shown for reverse unzipping.

Supplementary Table 1: Number of experiments for the data in Figs. 2 and 5

Context	site -1	site -2	site -3	consensus
C2	41	63	33	64
C1	213	47	78	41
C1 (reverse)	-	-	-	57
Lhb (forward)	140	140	140	-
Lhb (reverse)	63	63	63	-

Supplementary Table 2: Number of experiments for the data in Fig. 3

Mutation	Consensus	Site -1
3'-C	162	111
3'-G	183	331
3'-T	178	482
5'-A	83	180
5'-C	76	103
5'-T	51	120

Supplementary Table 3: Number of experiments for the data in Fig. 4

Nearest perturbed bp	Site -1	Nearest perturbed bp	Site -1
10	58	-1	73
11	26	-2	140
14	106	-3	75
15	108	-4	109
16	57	-5	86
18	218	-6	130
19	70	-8	109
20	72		

Supplementary Table 4: Number of experiments for the data in Supplementary Fig. 4

Concentration (nm)	8	17	31	62	125	250	500
Experiments	41	29	63	31	29	23	140

Supplementary Table 5: Calculated p-values for the data in Fig. 2

Breaking force

	Site 1			Site 2			Site 3			consensus	
	C2	C1	*Lhb*	C2	C1	*Lhb*	C2	C1	*Lhb*	C2	C1
C2		0.02	0.1		0.7	2E-08		0.7	1E-07		0.0007
C1			0.001			9E-07		1	8E-08		
Lhb										-	

Binding probability

	Site 1			Site 2			Site 3			consensus	
	C2	C1	*Lhb*	C2	C1	*Lhb*	C2	C1	*Lhb*	C2	C1
C2		0.01	0.007		5E-02	9E-02		0.02	0.8		0.1
C1			0.6			4E-04			0.001		
Lhb											

Supplementary Table 6: Calculated p-values for the data in Fig. 3

Binding probability, consensus

Mutation	C1	3'-C	3'-G	3'-T	5'-A	5'-C	5'-T
C1		0.2	0.5	0.007	0.3	0.01	0.1
3'-C			0.3	0.04	0.8	0.07	0.4
3'-G				0.004	0.5	0.02	0.2
3'-T					0.05	0.6	0.5
5'-A						0.06	0.4
5'-C							0.3
5'-T							

Binding probability, site -1

Mutation	C1	3'-C	3'-G	3'-T	5'-A	5'-C	5'-T
C1		1E-09	1E-09	1E-09	3E-05	0.005	0.5
3'-C			1E-01	0.1	1E-22	2E-14	2E-07
3'-G				0.7	1E-23	3E-14	6E-07
3'-T					1E-24	2E-14	6E-07
5'-A						0.4	5E-06
5'-C							0.001
5'-T							

Breaking force, consensus

Mutation	C1	3'-C	3'-G	3'-T	5'-A	5'-C	5'-T
C1		0.03	0.02	0.01	0.3	0.7	0.2
3'-C			0.4	0.7	0.05	0.001	0.1
3'-G				0.6	0.02	0.0005	0.08
3'-T					1E-02	0.0001	7E-02
5'-A						0.2	0.7
5'-C							0.1
5'-T							

Breaking force, site -1

Mutation	C1	3'-C	3'-G	3'-T	5'-A	5'-C	5'-T
C1		4E-11	7E-08	2E-43	1E-07	6E-08	4E-10
3'-C			0.04	1E-04	0.01	0.09	2E-01
3'-G				2E-18	0.6	0.7	2E-01
3'-T					8E-21	7E-13	2E-10
5'-A						0.4	0.1
5'-C							0.4
5'-T							

Supplementary Table 7: Calculated p-values for the data in Fig. 4

Breaking force, site -1, ZF1

Nearest perturbed bp	C1	-1	-2	-3	-4	-5	-6	-8
C1		5E-10	2E-08	0.0002	0.04	0.08	0.9	0.1
-1			0.1	5E-02	0.0003	0.0001	7E-08	1E-05
-2				0.3	0.005	0.002	1E-06	0.0003
-3					0.1	0.07	0.001	0.03
-4						0.7	0.07	0.5
-5							0.1	0.7
-6								0.1
-8								

Binding probability, site -1, ZF1

Nearest perturbed bp	C1	-1	-2	-3	-4	-5	-6	-8
C1		0.003	0.08	0.01	0.9	0.4	0.6	0.006
-1			5E-05	0.5	0.005	0.03	0.001	0.4
-2				0.0003	0.1	0.02	0.2	3E-05
-3					0.02	0.1	0.006	0.9
-4						0.4	0.5	0.01
-5							0.2	0.08
-6								0.002
-8								

Breaking force, site -1, ZF3

Nearest perturbed bp	C1	10	11	14	15	16	18	19	20
C1		3E-41	1E-26	1E-26	5E-28	2E-22	2E-34	2E-22	3E-29
10			0.001	5E-07	7E-07	1E-05	1E-20	2E-18	3E-22
11				0.1	0.1	0.2	9E-07	2E-07	2E-08
14					0.7	0.6	0.002	0.0001	0.0001
15						0.8	0.0004	3E-05	1E-05
16							0.001	0.0001	5E-05
18								0.09	0.1
19									0.6
20									

Binding probability, site -1, ZF3

Nearest perturbed bp	C1	3'\01	3'\02	3'\05	3'\06	3'\07	3'\09	3'\10	3'\11
C1		0.0001	0.9	0.6	0.5	0.4	0.4	0.9	0.4
10			3E-10	2E-09	2E-08	3E-07	7E-11	4E-10	4E-15
11				0.5	0.3	0.2	0.1	0.9	0.3
14					0.1	0.1	0.08	0.5	0.8
15						0.7	0.7	0.3	0.04
16							0.9	0.2	0.02
18								0.2	0.01
19									0.3
20									

Supplementary Table 8: Calculated KD for Egr-1 binding

Site	Context	KD (nM)
-1	*Lhb*	60 ± 20
-2	*Lhb*	440 ± 140
-3	*Lhb*	130 ± 90
Consensus	C-1	8 ± 6

Supplementary Table 9: Oligonucleotides used to synthesize the Lhb constructs.

Name	Sequence
mLh -517F BglI	ATGGCCTTGCCGGCGACACACCCCTTACTTCCAGAG
mLh +246R DraIII	ATCACTGCGTGTCTACCCCTGACCTGGTTTTTC

Supplementary Table 10: Oligonucleotides used to synthesize the C1 and C2 constructs.

Common reverse primer	601 R DraIII HP side	ATCACTGCGTGGTCACCGATGGACCCTATACG
Forward primers for WT	cons_5_prime_601_WT	ATGGCCTTGCCGGCcgcccacgcGATGTATATATCTGACACGTGCCTGGAGACTA
	site3_5_prime_601_WT	ATGGCCTTGCCGGCggcccactcGATGTATATATCTGACACGTGCCTGGAGACTA
	site2_5_prime_601_WT	ATGGCCTTGCCGGCcgcccccaaGATGTATATATCTGACACGTGCCTGGAGACTA
	site1_5_prime_601_WT	ATGGCCTTGCCGGCcacccccacGATGTATATATCTGACACGTGCCTGGAGACTA
	cons_601_WT	ATGGCCTTGCCGGCGATGTATATATCTGACACGcgcccacgcACTAGGGAGTAATCCCCTTG
	site3_601_WT	ATGGCCTTGCCGGCGATGTATATATCTGACACGggcccactcACTAGGGAGTAATCCCCTTG
	site2_601_WT	ATGGCCTTGCCGGCGATGTATATATCTGACACGcgcccccaaACTAGGGAGTAATCCCCTTG
	site1_601_WT	ATGGCCTTGCCGGCGATGTATATATCTGACACGcacccccacACTAGGGAGTAATCCCCTTG
Forward primers for single mutations	site1_601_3flankT	ATGGCCTTGCCGGCGATGTATATATCTGACACGcacccccacTCTAGGGAGTAATCCCCTTG
	site1_601_3flankC	ATGGCCTTGCCGGCGATGTATATATCTGACACGcacccccacCTAGGGAGTAATCCCCTTG
	site1_601_3flankG	ATGGCCTTGCCGGCGATGTATATATCTGACACGcacccccacGCTAGGGAGTAATCCCCTTG
	site1_601_5flankT	ATGGCCTTGCCGGCGATGTATATATCTGACACTcacccccacACTAGGGAGTAATCCCCTTG
	site1_601_5flankC	ATGGCCTTGCCGGCGATGTATATATCTGACACCcacccccacACTAGGGAGTAATCCCCTTG
	site1_601_5flankA	ATGGCCTTGCCGGCGATGTATATATCTGACACAcacccccacACTAGGGAGTAATCCCCTTG
	cons_601_3flankT	ATGGCCTTGCCGGCGATGTATATATCTGACACGcgcccacgcTCTAGGGAGTAATCCCCTTG
	cons_601_3flankC	ATGGCCTTGCCGGCGATGTATATATCTGACACGcgcccacgcCCTAGGGAGTAATCCCCTTG
	cons_601_3flankG	ATGGCCTTGCCGGCGATGTATATATCTGACACGcgcccacgcGCTAGGGAGTAATCCCCTTG

	cons_601_5flankT	ATGGCCTTGCCGGCGATGTATATATCTGACACTcgcccacgcACTAGGGAG TAATCCCCTTG
	cons_601_5flankC	ATGGCCTTGCCGGCGATGTATATATCTGACACCcgcccacgcACTAGGGAG TAATCCCCTTG
	cons_601_5flankA	ATGGCCTTGCCGGCGATGTATATATCTGACACAcgcccacgcACTAGGGAG TAATCCCCTTG
Forward primers for multiple mutations	site1_5flanKO8	ATGGCCTTGCCGGCGATGTATATATATGACACGcacccccacACTAGGGAG TAATCCCCTTG
	site1_5flanKO6	ATGGCCTTGCCGGCGATGTATATATATAACACGcacccccacACTAGGGAG TAATCCCCTTG
	site1_5flanKO5	ATGGCCTTGCCGGCGATGTATATATATATCACGcacccccacACTAGGGAG TAATCCCCTTG
	site1_5flanKO4	ATGGCCTTGCCGGCGATGTATATATATATAACGcacccccacACTAGGGAG TAATCCCCTTG
	site1_5flanKO3	ATGGCCTTGCCGGCGATGTATATATATATATCGcacccccacACTAGGGAG TAATCCCCTTG
	site1_5flanKO2	ATGGCCTTGCCGGCGATGTATATATATATATAGcacccccacACTAGGGAG TAATCCCCTTG
	site1_5flanKO1	ATGGCCTTGCCGGCGATGTATATATATATATATcacccccacACTAGGGAG TAATCCCCTTG
	site1_3flanKO11	ATGGCCTTGCCGGCGATGTATATATCTGACACGcacccccacACTAGGGAG TTATCCCCTTGGCGGTTAAAA
	site1_3flanKO10	ATGGCCTTGCCGGCGATGTATATATCTGACACGcacccccacACTAGGGAG ATATCCCCTTGGCGGTTAAAA
	site1_3flanKO9	ATGGCCTTGCCGGCGATGTATATATCTGACACGcacccccacACTAGGGAT ATATCCCCTTGGCGGTTAAAA
	site1_3flanKO7	ATGGCCTTGCCGGCGATGTATATATCTGACACGcacccccacACTAGGTAT ATATCCCCTTGGCGGTTAAAA
	site1_3flanKO6	ATGGCCTTGCCGGCGATGTATATATCTGACACGcacccccacACTAGATAT ATATCCCCTTGGCGGTTAAAA
	site1_3flanKO5	ATGGCCTTGCCGGCGATGTATATATCTGACACGcacccccacACTATATAT ATATCCCCTTGGCGGTTAAAA
	site1_3flanKO2	ATGGCCTTGCCGGCGATGTATATATCTGACACGcacccccacAATATATAT ATATCCCCTTGGCGGTTAAAA
	site1_3flanKO1	ATGGCCTTGCCGGCGATGTATATATCTGACACGcacccccacTATATATAT ATATCCCCTTGGCGGTTAAAA

Supplementary Table 11: Oligonucleotides used to synthesize the dsDNA handles and alignement segment.

2k BioTg F	GATCTCCAGCCAGGAACTATTGA
2k bio R Nt.BvCI	GTGTCAGCTTGCCCCTCAGCGATGACCTCAGCATTTTTCGACCTGCTCTTCAGCA
2K DoubleDig2 bgl1F	ATGGCCTAGACGGCGAGCCTGGGTTTATAAGGGGAGCGGTGA
2k Dig Nb.BbVCI R	TCAGCTTGCCCCTCAGCGATGACCTCAGCAAGGACCAGCGTTTTGTTGAAA
Oligo 5' Dig AGA	AGGTGCCGGGACCACCCTGTAGA
Oligo 3' Dig/ 5' phosphate	ACAGGGTGGTCCCGGCACCT
Alignment F DraIII CAC	ATCACCACGTGGAATTCGATATCCCCGAGA
Alignment R DraIII	ATGCACGCAGTGACCATGGTGGTGTTTCCC
Hairpin oligo 5' phos	GACTTGAGGCAATTGCCTCAAGTCtgc

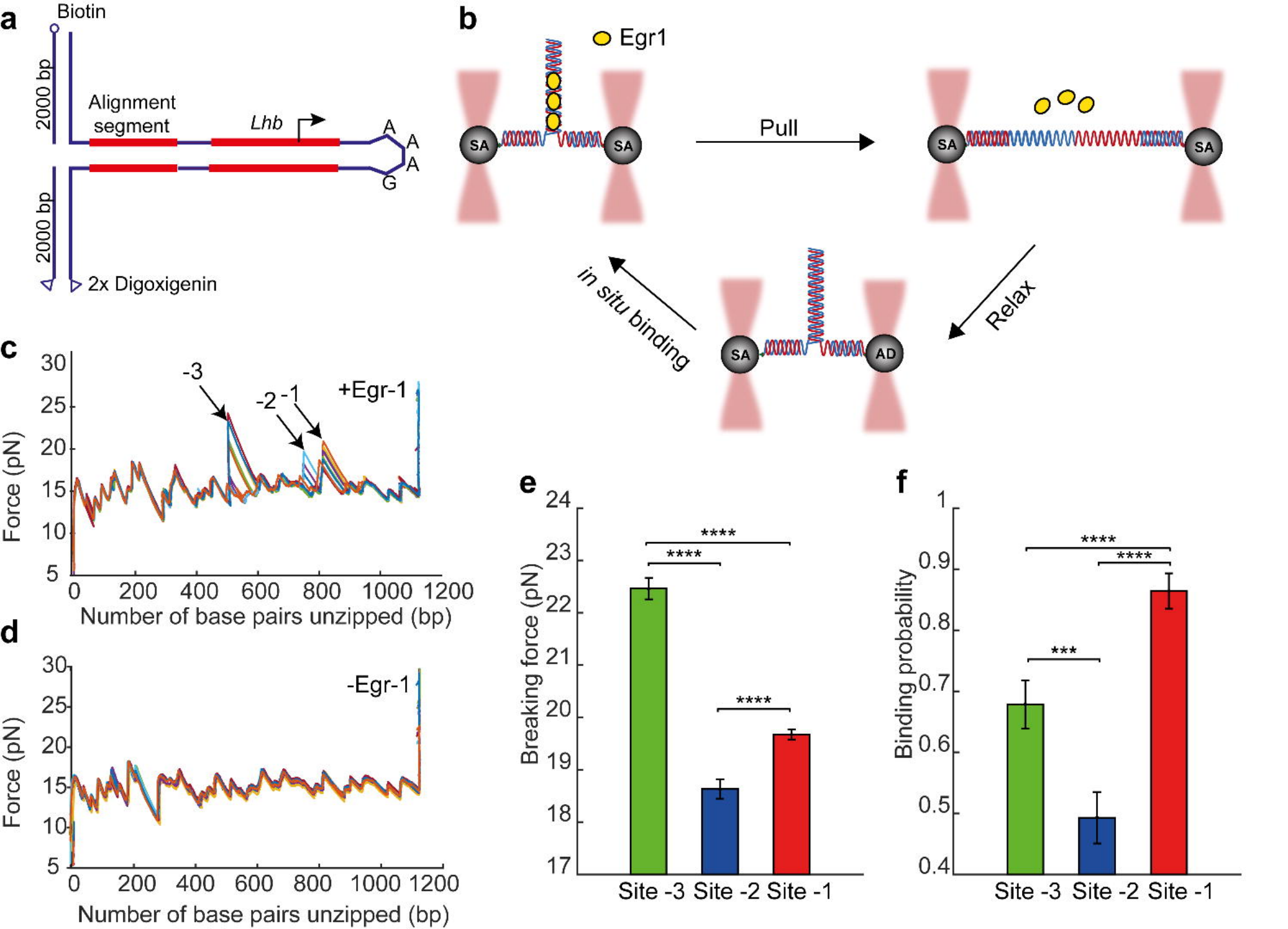
a
Biotin
2000 bp
Alignment segment
Lhb
A
A
A
G
2000 bp
2x Digoxigenin
b
Egr1
SA
SA
Pull
SA
SA
Relax
SA
AD
in situ binding
c
+Egr-1
-3
-2
-1
Force (pN)
Number of base pairs unzipped (bp)
d
-Egr-1
Force (pN)
Number of base pairs unzipped (bp)
e
Breaking force (pN)
****
****
****
Site -3
Site -2
Site -1
f
Binding probability
****
****
***
Site -3
Site -2
Site -1